An Adaptive Control Algorithm for Maximum Power Point Tracking for Wind Energy Conversion Systems

by

Joanne Hui

A thesis submitted to the
Department of Electrical and Computer Engineering
in conformity with the requirements for
the degree of Master of Science (Engineering)

Queen's University
Kingston, Ontario, Canada
December 2008

Abstract

Wind energy systems are being closely studied because of its benefits as an environmentally friendly and renewable source of energy. Because of its unpredictable availability, power management concepts are essential to extract as much power as possible from the wind when it becomes available.

The purpose of this thesis is to presents a new adaptive control algorithm for maximum power point tracking (MPPT) in wind energy systems. The proposed control algorithm allows the generator to track the optimal operation points of the wind turbine system under fluctuating wind conditions and the tracking process speeds up over time. This algorithm does not require the knowledge of intangible turbine mechanical characteristics such as its power coefficient curve, power characteristic or torque characteristic. The algorithm uses its memory feature to adapt to any given wind turbine and to infer the optimum rotor speeds for wind speeds that have not occurred before. The proposed algorithm uses a modified version of Hill Climb Search (HCS) and intelligent memory to implement its power management scheme. This algorithm is most suitable for smaller grid or battery connected wind energy systems. PSIM simulation studies have been done to confirm the effectiveness of the proposed algorithm.

Acknowledgments

First and foremost I would like to thank my supervisor Dr. Alireza Bakhshai for his wisdom and guidance. Secondly I would like to thank my mom, Rosalind Li, for giving me unconditional love and support throughout my academic career. I would also like to thank all the professors that have taught me throughout my years at Queen's. Lastly, for their advice, support and laughter, I would like to acknowledge all of my fellow ePEARL colleagues; special thanks to John, Ali and Majid.

Glossary

C_p	Power Coefficient
β	Pitch Angle
t_m	Turbine Mechanical Torque
p_m	Turbine Mechanical Power
ω	Angular Speed
C_p	Power Coefficient
$C_{p,max}$	Power coefficient value that results in maximum power transfer
P_{out}	Output Power
V_{dc}	DC Link Voltage
I_f	Generator Field Current
I_g	Load Current
I_{dm}	Demanded Current
P_{dm}	Power Demanded
ω_{ref}	Reference Angular Speed
ω_{gen}	Generator Angular Speed
λ_{opt}	Optimal Tip-Speed Ratio

v_w	Wind Velocity
ω_{opt}	Optimal Angular Speed
G	Gear Ratio
R	Turbine Blade Radius
L_{max}	Maximum Boost Converter Inductor Value
C_{min}	Mininmum Output Capacitor Value
d	Duty Ratio
MPPT	Maximum Power Point Tracking
HCS	Hill Climb Searching
WECS	Wind Energy Conversion System
TSR (λ)	Tip-Speed Ratio
CDL	Change Detection Loop
OPAL	Operating Point Adjustment Loop
WECS	Wind Energy Conversion System
WFSG	Wound Field Synchronous Generator
SCIG	Squirrel Cage Induction Generator
PWM	Pulse Width Modulation
PMSG	Permanent Magnet Synchronous Generator
DFIG	Doubly Fed Wound Rotor Induction Generator
AHCS	Advanced Hill Climb Search
MPED	Max-Power Error Driven
DCM	Discontinuous Conduction Model

FPGA Field Programmable Gate Array

DSP Digital Signal Processor

Table of Contents

List of Tables

List of Figures

Chapter 1

Introduction

Due to the increasing concern about the environment and the depletion of natural resources such as fossil fuels, much research is now focused on obtaining new environmentally friendly sources of power. To preserve our planet for the future generations, natural renewable sources are being closely studied and harvested for our energy needs. Wind energy is environmentally friendly, inexhaustible, safe, and capable of supplying substantial amounts of power. However, due to wind's erratic nature, intelligent control strategies must be implemented to harvest as much potential wind energy as possible while it is available. Because of its advantages, erratic nature, and recent technological advancements in wind turbine aerodynamics and power electronic interfaces, wind energy is considered to be an excellent supplementary energy source. Research to extract the maximum power out of wind energy is an essential part of making wind energy much more viable and attractive.

1.1 Wind Energy Market

Wind energy has been harnessed by many generations for thousands of years to mill grain, pump water and sailing [9]. It wasn't until the late nineteen century when the development of a 12 kW windmill generator was used to generate electricity [9]. However, it was only in the 1980s that the technology has become mature enough to efficiently and reliably produce electricity. Since then, many wind energy systems have been developed and the technological advances have been phenomenal. Just in last decade, the wind energy industry has experienced a growth of almost 30 percent each year [2]. The global value of new wind energy plants installed in 2006 alone has reached US $24 billion, and over 70 countries have wind turbine installations [2]. From 1996 to 2007, the total cumulative capacity of global wind power has increased from 6.8 GW to 93.8 GW (See Figure 1.1) [1]. In particular, the last two years (2006 and 2007) have been record breaking years for the wind industry. Before 2007, 2006 had the highest ever amount of installations of wind energy systems in a single year, reaching 15 GW (See Figure 1.2) [2]. Afterwards, the year 2007 became another historical year as the total cumulative capacity of global wind power increased by 19.8 GW (27% growth) to reach a final total of 93.8 GW of installed wind power (See Figure 1.2) [1].

Figure 1.3a and 1.3b show the distribution of the top ten countries with the highest percentage of installed wind energy conversion systems (WECS) and the top ten countries with the highest percentage of newly installed WECSs in 2006 respectively.

Not only is wind energy environmentally friendly, its development also strengthens local economies and insulates the countries from macro-economical shocks of the global commodities market (volatile gas, oil and coal prices) [2]. With continuous

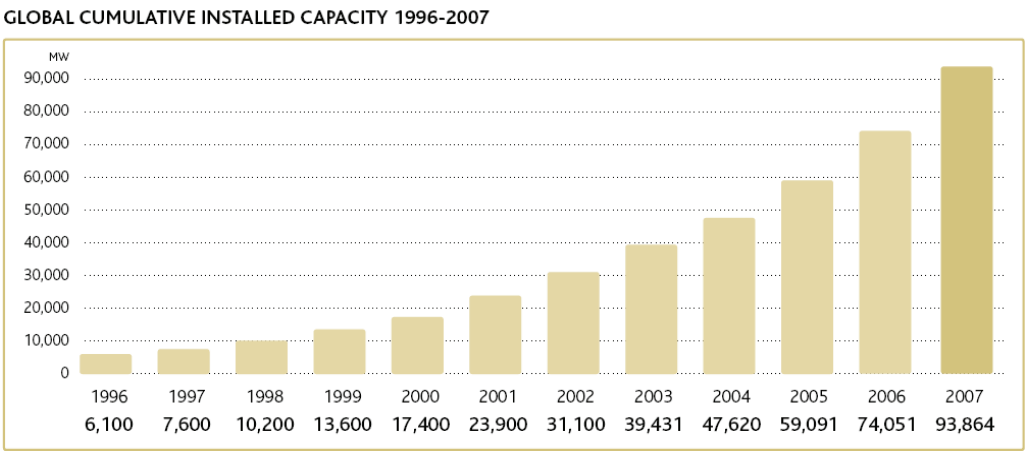

Figure 1.1: the total amount of globally installed wind energy systems per year [1].

cost reductions in wind turbines, government incentive programs promoting wind energy, and public demand for cleaner power sources, wind energy has become one of the most promising and fastest growing energy resources in the world. As of 2006, North America (mainly US and Canada), accounts for approximately 17.6% of the global wind power installations [9]. With an 113% increase in new installations from 2005, 2006 was the most significant year for the wind industry in Canada. In 2006, Canada was ranked 12th in the world with a total of 1.46 GW of installed wind power, and ranked 7th for having a 0.78 GW of new installations [2]. As the interest in wind energy continues, Canada has experienced its second best year in 2007 with a 26% increase (386 MW) in new wind energy capacity [1]. As of 2007, Canada now has 1846 MW of installed wind energy capacity and it is now ranked 10th in terms of new installations (See Figure 1.4). As of 2008, Canada has signed contracts for the installation of an additional 2.8 GW of wind energy by 2010. The Canadian government hopes to have at least 10 GW of installed wind power by 2015. This translates to a reduction of 12 million tons of greenhouse gas emissions [9]. Also

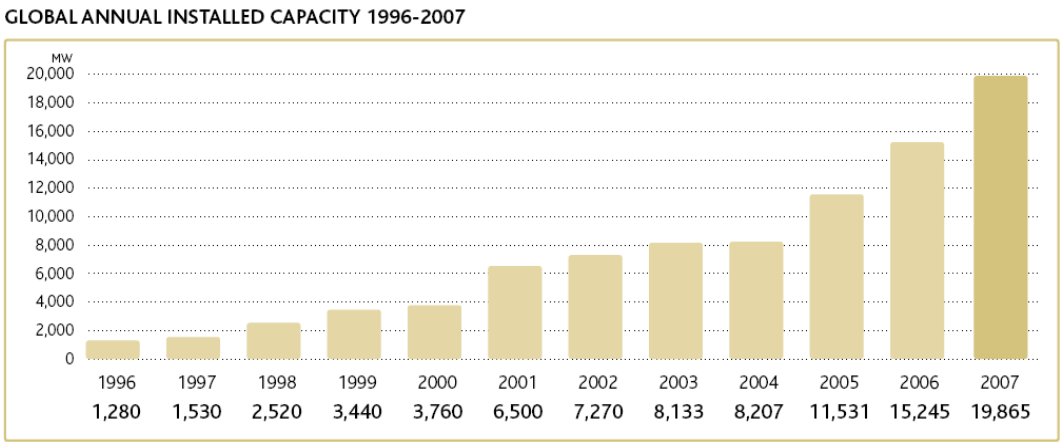

Figure 1.2: the total amount of the newly installed wind energy systems around the world per year [1].

because of the geographical nature of the nation, Canada has more than enough wind resources to meet 20% of its population's electricity demand [10].

1.2 Wind Energy Conversion Principles

The classical equations of kinetic energy and power describe the potential energy that can be harnessed from the wind. The kinetic energy available from wind is described by (1.1) [11]. By classical physics theory, to translate kinetic energy into the power, energy is divided by time; thus the power from the kinetic energy is given by (1.2).

$$E_k = 0.5mv_w^2 = 0.5\rho A d v_w^2 \tag{1.1}$$

$$p_w = \frac{0.5mv_w}{t} = \frac{0.5\rho A d v_w^2}{t} = 0.5\rho A v_w^3 \tag{1.2}$$

Where ρ = air density, A = rotor swept area, d = distance, m = mass of air = air density * volume = ρ*A*d, and V_w = distance/time.

With the theoretical power available in wind established by (1.1) and (1.2), the

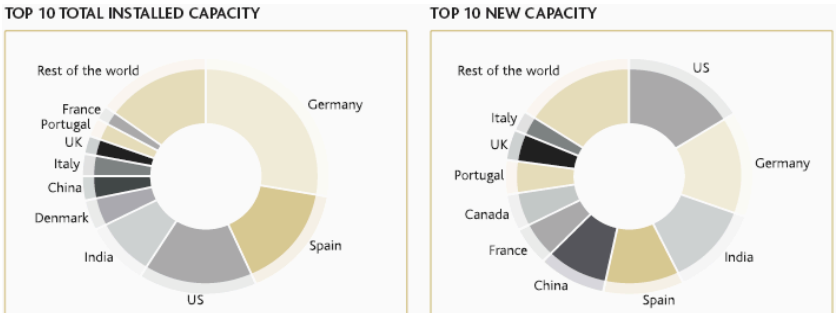

	MW	%
Germany	20,622	27.8
Spain	11,615	15.6
US	11,603	15.6
India	6,270	8.4
Denmark	3,136	4.2
China	2,604	3.5
Italy	2,123	2.9
UK	1,963	2.6
Portugal	1,716	2.3
France	1,567	2.1
Rest of the world	11,005	14.8
Total top 10	**63,218**	**85.2**
Total	**74,223**	

(a)

	MW	%
US	2,454	16.1
Germany	2,233	14.7
India	1,840	12.1
Spain	1,587	10.4
China	1,347	8.9
France	810	5.3
Canada	776	5.1
Portugal	694	4.6
UK	634	4.2
Italy	417	2.7
Rest of the world	2,405	15.8
Total top 10	**12,792**	**84.2**
Total	**15,197**	

(b)

Figure 1.3: a:Total installed WECS distribution (as of 2006); b:Newly installed WECS distribution(as of 2006) [2].

power extracted by wind turbines must be addressed since it is the first and foremost element of any wind energy conversion system (WECS). The aerodynamic efficiency of the turbine while converting wind into useable electrical power is described by its power coefficient, C_p, curve. The physical meaning of the C_p curve is the ratio of the actual power delivered by the turbine and the theoretical power available in the wind. A turbine's efficiency, and thus power coefficient curve, is what differentiates one turbine from another. By taking the efficiency of the turbine into account, (1.3) represents the mechanical power captured by the wind by any turbine.

$$p_m = 0.5\rho A C_p(\lambda, \beta) v_w^3 \tag{1.3}$$

Where $C_p(\lambda, \beta)$ = power coefficient function, λ = the tip speed ratio, and β =

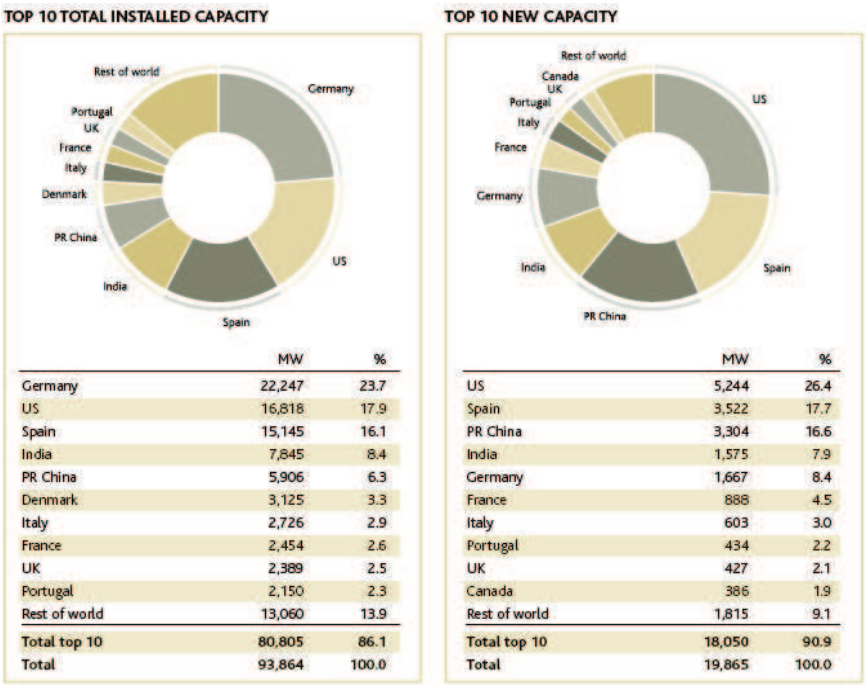

	MW	%
Germany	22,247	23.7
US	16,818	17.9
Spain	15,145	16.1
India	7,845	8.4
PR China	5,906	6.3
Denmark	3,125	3.3
Italy	2,726	2.9
France	2,454	2.6
UK	2,389	2.5
Portugal	2,150	2.3
Rest of world	13,060	13.9
Total top 10	80,805	86.1
Total	93,864	100.0

	MW	%
US	5,244	26.4
Spain	3,522	17.7
PR China	3,304	16.6
India	1,575	7.9
Germany	1,667	8.4
France	888	4.5
Italy	603	3.0
Portugal	434	2.2
UK	427	2.1
Canada	386	1.9
Rest of world	1,815	9.1
Total top 10	18,050	90.9
Total	19,865	100.0

Figure 1.4: a:Total installed WECS distribution (as of 2007); b:Newly installed WECS distribution(as of 2007) [1].

pitch angle.

From (1.3), it can be observed that the power available in the wind is proportional to the cube of the wind speed. This means that there is much more energy in high-speed winds than in slow winds. Also, since the power is proportional to the rotor swept area, and thus to the square of the diameter, doubling the rotor diameter will quadruple the available power. Air density also plays a role in the amount of available mechanical power of the turbine; lower air densities (e.g. warm air) results in less available power in wind. The power coefficient function, $C_p(\lambda, \beta)$, is dependent on two factors: i) the tip speed ratio (λ), and ii) the pitch angle (β). This function is normally provided (in the form of a curve) by the wind turbine manufacturer since it characterizes the efficiency of its wind turbines. If this curve is not provided, then it

can be obtained by performing field tests. The power coefficient can be evaluated by (1.4).

$$C_p(\lambda, \beta) = \frac{actualturbinepower}{theoreticalwindpower} = \frac{p_m}{p_w} = \frac{p_m}{0.5\rho A v_w^3} \tag{1.4}$$

The tip speed ratio (TSR), λ, refers to the ratio of the turbine angular speed over the wind speed. The mathematical representation of the tip speed ratio is given to be as follows [6]:

$$\lambda = \frac{R\omega_b}{v_w} \tag{1.5}$$

The pitch angle, β, on the other hand, refers to the angle at which the turbine blades are aligned with respect to its longitudinal axis. From a mechanical control point of view, the pitch angle can be controlled in such a way so that the maximum power from the wind is extracted. For example, if the wind velocity exceeds that of the rated system, then the rotor blades would be 'pitched' (angled) out of the wind, and when the wind is below that of the rated system, the rotor blades would be 'pitched' back into the wind [12]. This mechanism is implemented by means of hydraulics systems. There are systems where the variable pitch control is not implemented. In these cases, the C_p functions for those wind turbines depend only on the tip speed ratio. A typical C_p curve with a fixed pitch angle is illustrated by Figure 1.5 [6].

Since the air density and rotor swept area in (1.1) can be considered constant, the power curves for each wind speed are only influenced by the C_p curve. Thus, it can be seen in Figure 1.6 that the shape of the power characteristic is similar to the C_p curve in Figure 1.5. Also from Figure 1.6, it should be noted that the point at which maximum power occurs for each wind speed is different and distinct. The turbine

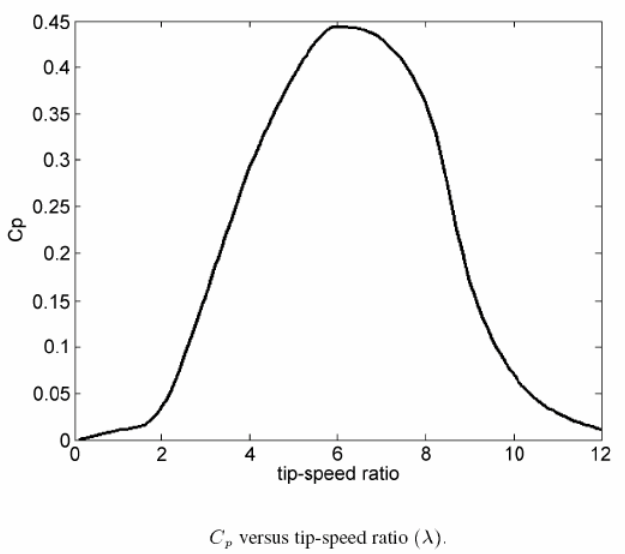

Figure 1.5: A typical power coefficient curve of a fixed-pitch wind turbine.

mechanical torque is as follows [6].

$$t_m = p_m \frac{R}{G\lambda v_w} \tag{1.6}$$

Where R = turbine radius, and G = speed-up gear ratio.

Equation (1.6) shows that the mechanical torque produced by the turbine is a function of the mechanical power, tip speed ratio, gear ratio, turbine radius, and wind speed. By substituting (1.3) and (1.5), the equations describing the power and tip speed ratio respectively, into (1.6) we get:

$$t_m = 0.5\rho A C_p(\lambda, \beta) \frac{R}{G v_w} \tag{1.7}$$

After simplification (1.7) becomes:

$$t_m = \frac{0.5\rho A C_p(\lambda, \beta) v_w}{G\omega} = \frac{p_m}{G\omega} \tag{1.8}$$

From (1.8) it can be seen that the mechanical torque available from the wind turbine is the same as the classical physics equation of torque (t_m) and power (p_m) where $p_m = t_m$*angular velocity (ω). Like the power characteristic, it should also

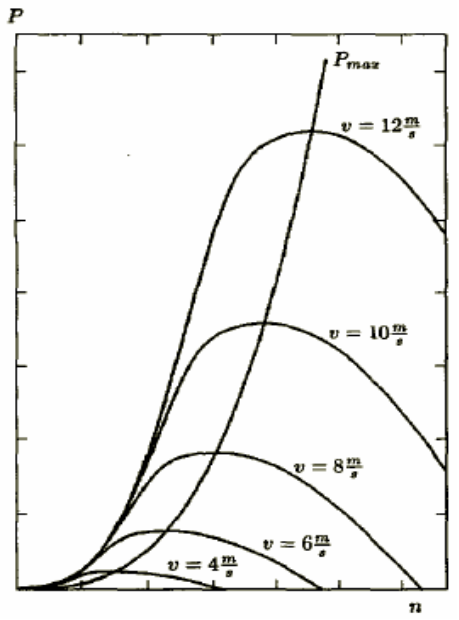

Figure 1.6: The power characteristic of a typical wind turbine (this curve illustrates (1.3)). The trajectory labelled P_{max} represents the maximum points on the power curves[3].

be noted that the shape of the torque curve is characterized by the power coefficient (C_p). As a result, the peak torque will also correspond to a particular rotor speed. Because the torque is the mechanical power divided by a constant gear ratio and the angular speed of the turbine, the shape of the curve is very similar to the power curve. Their peaks however, do not correspond to the same rotor speed. Therefore, the rotor speed that gives maximum torque does not correspond to the rotor speed that gives maximum power.

1.3 Concept of Maximum Power Extraction

Normal wind energy conversion is relatively straightforward process, but in order to capture the maximum power from the wind, the process is much more involved.

It can be observed from Figure 1.6 that the maximum of the power curve, for a particular wind speed, occurs at a particular rotor speed. Due to the aerodynamic characteristics of a wind turbine, a small variation from the optimum rotor speed will cause a significant decrease in the power extracted from the wind. Turbines do not naturally operate at the optimum wind speed for any given wind velocity because its rotor speed is dependent on the generator loading as well as the wind speed fluctuations. Because of this, non-optimized conversion strategies lead to a large percentage of wasted wind power. The more energy extracted from the wind, the more cost effective the wind energy becomes.

Due to the aerodynamics of a wind turbine (dictated by the C_p function), the same turbine angular speed for different wind speeds will result in different levels of extracted power. Recall from Section 1.2 that the $C_{p,max}$ for a fixed pitched wind turbine corresponds to one particular TSR value (See Figure 1.5). Because the TSR is a ratio of the wind speed and the turbine angular rotational speed, the optimum speed for maximum power extraction is different for each wind speed [6][13], but the optimum TSR value remains the same. As an example, figure 1.7 and 1.8 are the power and torque characteristics of the wind turbine used in this study. The power and torque characteristics illustrated by Figure 1.7 and Figure 1.8 are similar to the characteristics of typical fixed pitch wind turbines. Fixed-speed wind turbine systems will only operate at its optimum point for one wind speed [14]. So to maximize the amount of power captured by the turbine, variable-speed wind turbine systems are used because they allow turbine speed variation [6][14][7][3][15][16][17]. Power extraction strategies assesses the wind conditions and then forces the system to adjust the turbine's rotational speed through power electronic control and/or mechanical

devices so that it will operate at the turbine's highest aerodynamic efficiency. The primary challenge of wind energy systems is to be able to capture as much energy as possible from the wind in the shortest time. From the electronics point of view, this goal can be achieved through different converter topologies and maximum power point tracking (MPPT) algorithms.

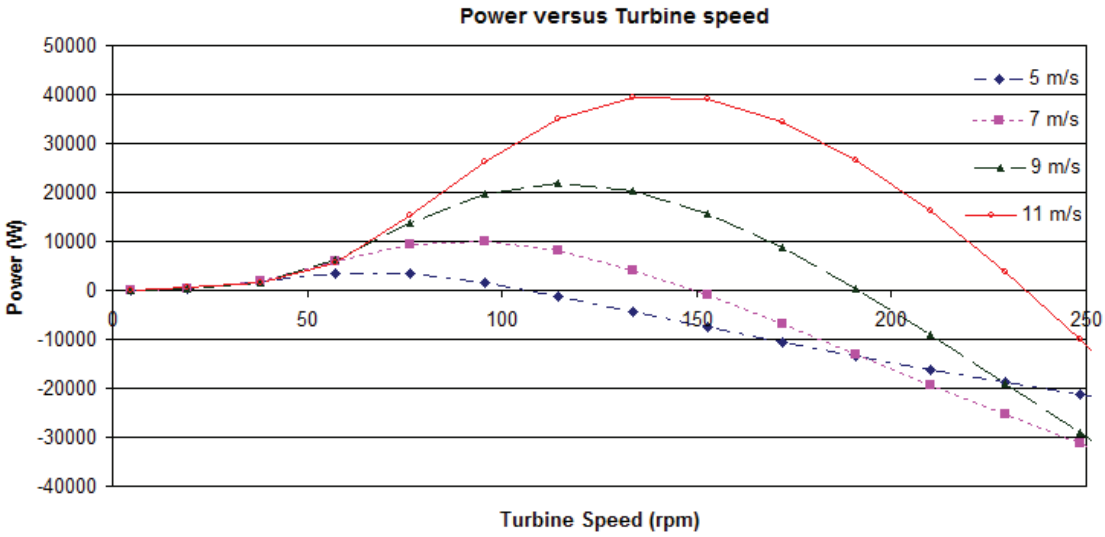

Figure 1.7: Example: The power characteristic of the wind turbine used in this study.

1.4 Concept of Proposed Algorithm

The proposed algorithm in this thesis takes an initial guess for the optimum TSR and subsequently uses it to calculate the starting reference signal. The system is then adjusted towards the optimum point by using a modified version of HCS (hill climb searching). Once an optimum point has been determined, it is stored and used when the corresponding wind speed occurs again to speed up the determination process. The algorithm also automatically determines a more accurate tip speed ratio for the

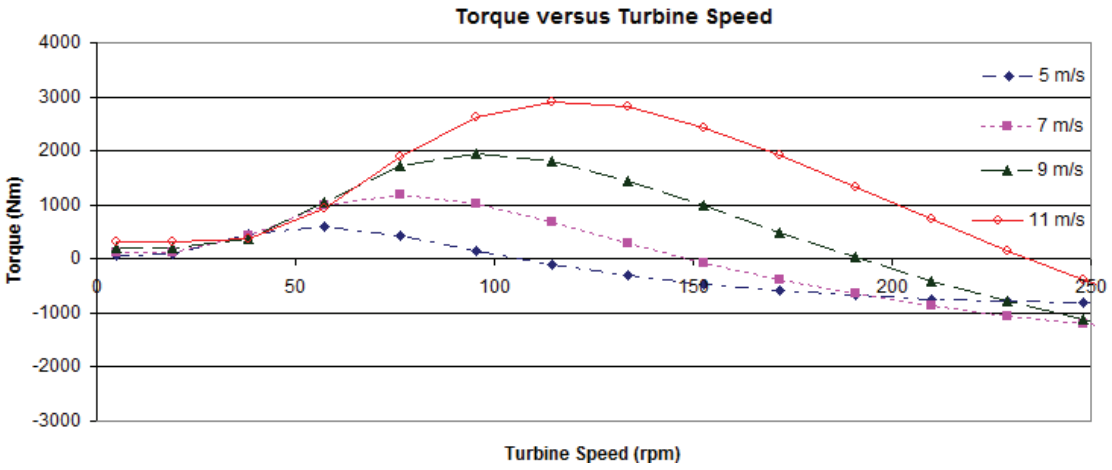

Figure 1.8: Example: The torque characteristic of the wind turbine used in this study.

turbine each time an optimum point is found. The establishment of the determined tip speed ratio facilitates more accurate estimations of the optimum operating point for wind speeds that have not yet occurred. The algorithm requires the turbine blade radius and gear ratio, but they are easy to obtain parameters so it can be easily configured to adapt to any turbine. These features of the proposed algorithm allow it to be fast, effective, and flexible.

1.5 Organization of Thesis

The organization of this thesis is outlined as follows:

Chapter 1 provided some general background information regarding the motivations for wind energy research, basic wind energy conversion principles, and the basic idea behind maximum wind power extraction. The general concept of the proposed maximum power extraction algorithm was also presented.

Chapter 2 gives an overview of wind turbine technology and wind energy conversion system configurations. The advantages and disadvantages of the different types of wind turbines and the two main kinds of wind energy systems are discussed. Power electronic interfaces and the roles of the converters are examined in this chapter. Lastly, a literature review of existing maximum power point tracking techniques is presented along with their strengths and weaknesses.

Chapter 3 describes the proposed maximum power point tracking control algorithm in detail. The algorithm features, overall concept, structure and implementation are discussed.

Chapter 4 discusses the modelling of each component in the wind energy conversion system considered in this thesis. The turbine model, turbine-generator shaft, and the boost converter design are described in this chapter. This chapter also deals with the boost converter stability analysis and the compensator design for the closed loop verification for the proposed algorithm.

Chapter 5 uses the simulated wind energy system to systematically verify the algorithm's functionality. The algorithm was subjected to through various wind conditions in order to confirm the effectiveness of the proposed control method.

Chapter 6 summarizes all the features ad contributions of the proposed maximum power point tracking algorithm. It also provides suggestions on the future works that can be done.

Chapter 2

Wind Energy Conversion Systems

2.1 Wind Turbine Technology

The wind turbine is the first and foremost element of wind power systems. There are two main types of wind turbines, the horizontal-axis and vertical-axis turbines.

2.1.1 Horizontal-axis Turbines

Horizontal-axis turbines (see Figure 2.1) are primarily composed of a tower and a nacelle mounted on top of tower. The generator and gearbox are normally located in the nacelle. It has a high wind energy conversion efficiency, self-starting capability, and access to stronger winds due to its elevation from the tower. Its disadvantages, on the other hand, include high installation cost, the need of a strong tower to support the nacelle and rotor blade, and longer cables to connect the top of the tower to the ground [9].

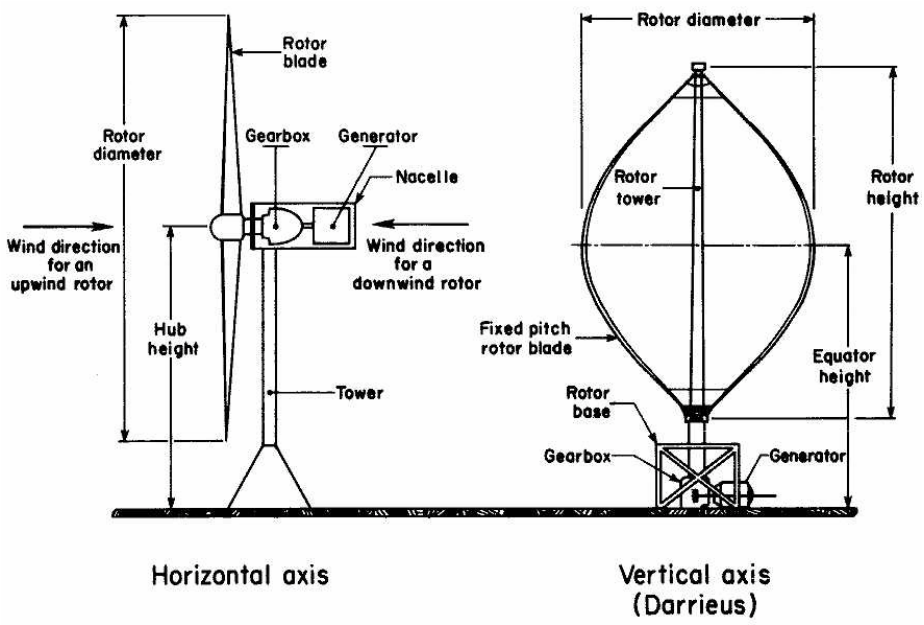

Figure 2.1: illustration of a horizontal axis and a vertical axis wind turbine [4].

2.1.2 Vertical-axis Turbines

A vertical axis turbines' spin axis is perpendicular to the ground (See Figure 2.1) [9]. The wind turbine is vertically mounted, and its generator and gearbox is located at its base [9]. Compared to horizontal-axis turbines, it has reduced installation cost, and maintenance is easier, because of the ground level gear box and generator installation [18]. Another advantage of the vertical axis turbine is that its operation is independent of wind direction [18]. The blades and its attachments in vertical axis turbines are also lower in cost and more rugged during operation. However, one major drawback of the vertical wind turbine is that it has low wind energy conversion efficiency and there are limited options for speed regulation in high winds [9]. Its efficiency is around half of the efficiency of horizontal axis wind turbines [9]. Vertical axis turbines also have high torque fluctuations with each revolution, and are not self-starting [9]. Mainly

due to efficiency issue, horizontal wind turbines are primarily used. Consequently, the wind turbine considered in this thesis is a horizontal axis turbine.

2.2 Types of Horizontal-Axis Wind Turbines

2.2.1 Pitched Controlled Wind Turbines

Pitch controlled wind turbines change the orientation of the rotor blades along its longitudinal axis to control the output power. These turbines have controllers to check the output power several times per second, and when the output power reaches a maximum threshold, an order is sent to the blade hydraulic pitch mechanism of the turbine to pitch (or to turn) the rotor slightly out of wind to slow down the turbine. Conversely, when the wind slows down, then the blades are turned (or also known as pitched) back into the wind. During operation, the blades are pitched a few degrees with each change in wind to keep the rotor blades at the optimum angle to maximum power capture. [12]

2.2.2 Stalled Controlled Wind Turbines

The rotor blades of a stall controlled wind turbine are bolted onto the hub at a fixed angle. The blades are aerodynamically designed to slow down the blades when winds are too strong. The stall phenomenon caused by turbulence on rotor blade prevents the lifting force to act on the rotor. The rotor blades are twisted slightly along the longitudinal axis so that the rotor blade stalls gradually rather than suddenly when the wind reaches the turbines' critical value.[12]

2.2.3 Active Stall Controlled Wind Turbines

Active stall turbines are very similar to the pitch controlled turbine because they operate the same way at low wind speeds. However, once the machine has reached its rated power, active stall turbines will turn its blades in the opposite direction from what a pitch controlled machine would. By doing this, the blades induces stall on its rotor blades and consequently waste the excess energy in the wind to prevent the generator from being overloaded. This mechanism is usually either realized by hydraulic systems or electric stepper motors. [12]

2.3 Types of Wind Energy Conversion Systems (WECS)

There are two main types of WECSs, the fixed speed WECS and variable-speed WECS. The rotor speed of a fixed-speed WECS, also known as the Danish concept, is fixed to a particular speed. The other type is the variable-speed WECS where the rotor is allowed to rotate freely. The variable-speed WECS uses power maximization techniques and algorithms to extract as much power as possible from the wind.

2.3.1 Fixed Speed Wind Energy Conversion Systems

As the name suggests, fixed speed wind energy systems operate at a constant speed. The fixed speed WECS configuration is also known as the "Danish concept" as it is widely used and developed in Denmark [19]. Normally, induction (or asynchronous) generators are used in fixed speed WECSs because of its inherent insensitivity to changes in torque [2] [12]. The rotational speed of an induction machine varies with

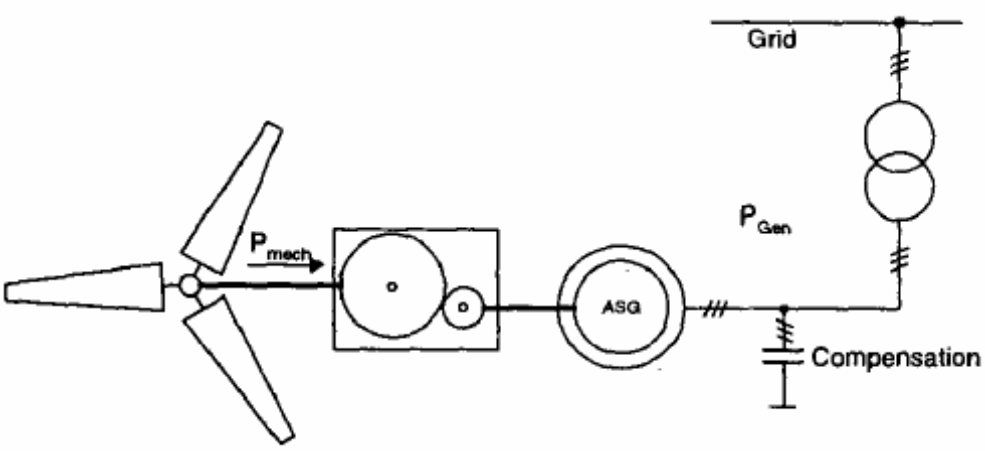

Figure 2.2: A typical fixed speed wind turbine configuration [5].

the force applied to it, but in practice, the difference between its speed at peak power and at idle mode (at synchronous speed) is very small [2]. The fixed speed wind systems have the generator stator directly coupled to the grid (see Figure 2.2). Consequentially, the system is characterized by stiff power train dynamics that only allow small variations in the rotor speed around the synchronous speed. Due to the mechanical characteristics of the induction generator and its insensitivity to changes in torque, the rotor speed is fixed at a particular speed dictated by the grid frequency, regardless of the wind speed [19]. The construction and performance of fixed-speed wind turbines are dependent on the turbine's mechanical characteristic [14].

Squirrel-cage induction generators (SCIG) are typically used in fixed speed systems [19] [20]. The system in Figure 2.2 transforms wind energy into electrical energy by using a squirrel cage induction machine directly connected to a three-phase power grid [5]. The rotor of the wind turbine is coupled to the generator shaft with a fixed ratio gearbox [5].

With respect to variable speed wind turbines, fixed speed turbines are well established, simple, robust, reliable, cheaper, and maintenance-free [9] [19] [20]. But because the system is fixed at a particular speed, variation in wind speed will cause the turbine to generate highly fluctuating output power to the grid [6], [9]. These load variations require a stiff power grid to enable stable operation and the mechanical design must be robust enough to absorb high mechanical stresses [5] [20]. Also, since the turbine rotates at a fixed speed, maximum wind energy conversion efficiency can be only achieved at one particular wind speed [6], [9]. This is because for each wind speed, there is a particular rotor speed that will produce the TSR that gives the maximum C_p value. As observed from the relationship described by (1) and illustrated by Figures 1.5 and 1.6, the maximum C_p value corresponds to the maximum mechanical power. Since fixed speed systems do not allow significant variations in rotor speed, these systems are incapable of achieving the various rotor speeds that result in the maximum C_p value under varying wind conditions.

2.3.2 Variable Speed Wind Turbine Systems

In variable speed wind turbine systems, the turbine is not directly connected to the utility grid. Instead, a power electronic interface is placed between the generator and the grid to provide decoupling and control of the system. Thus, the turbine is allowed to rotate at any speed over a wide range of wind speeds [6], [9]. It has been discussed earlier that each wind speed has a corresponding optimal rotor speed for maximum power. With the added control feature of variable speed systems, they are capable of achieving maximum aerodynamic efficiency [9]. By using control algorithms and/or mechanical control schemes (i.e. pitch controlled, etc), the turbine can programmed

to extract maximum power from any wind speed by adjusting its operating point to achieve the TSR for maximum power capture. The mechanical stresses on the wind turbine are reduced since gusts of wind can be absorbed (i.e. energy is stored in the mechanical inertia of the turbine and thus reduces torque pulsations) [6], [9], [5]. Another advantage of this system is that the power quality can be improved by the reduction of power pulsations due to its elasticity [6], [5]. The disadvantages of the variable speed system include the additional cost of power converters and the complexity of the control algorithms [6], [9]. In this thesis, an adaptive maximum power point tracking control algorithm is developed for variable speed energy systems to achieve maximum efficiency under fluctuating wind conditions.

2.4 Configurations of Variable Speed Wind Conversion Systems

2.4.1 Synchronous Generators

The stator of the synchronous generators holds the set of three-phase windings that supply the external load. The rotor, on the other hand, is the source of the machine's magnetic field. The magnetic field is either supplied by a direct current (DC) flowing in a wound field or a permanent magnet.

Figure 2.3 illustrates a typical setup of a wind turbine with a wound field synchronous generator (WFSG) connected to the grid through power electronic converters. The WFSG has high machine efficiency, and the power electronic converters allow direct control over the power factor. However, because of the winding circuit in

the rotor, the size of the WFSG can be rather large. Another drawback of the configuration in Figure 2.3 is that in order to regulate the active and reactive power, the power electronic converter must be sized typically 1.2 times the rated power. Thus, the use of the WFSG leads to a bulky system. [6]

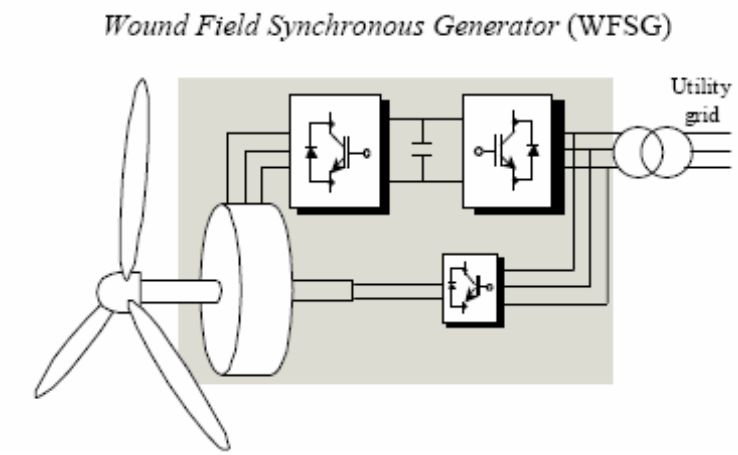

Figure 2.3: A typical fixed speed wind turbine configuration [5].

In Figure 2.3, the stator of the turbine is connected to the utility grid through two back-to-back pulse width modulated (PWM) converters. The main task of the stator side converters is to control the electromagnetic torque of the turbine. By adjusting the electromagnetic torque, the turbine can be forced to extract maximum power. The rectifier connects the rotor and the utility; it converts the alternating current (AC) from the utility grid into a direct current into the rotor windings. DC current flows through the rotor windings and supplies the generator with the necessary magnetic field for operation.

Permanent magnet synchronous generators (PMSG) are common in low power, variable speed wind energy conversion systems [11]. The advantages of using PMSGs are its high efficiency and small size. However, the cost of the permanent magnet

and the demagnetization of the permanent magnet material should be considered [6]. Figure 2.4 and 2.5 illustrate two common grid connection configurations of PMSG wind turbines.

In Figure 2.4, the stator windings are connected to the utility grid through a diode rectifier, boost converter, and a PWM inverter. The diode rectifier rectifies the variable frequency and magnitude output AC voltages from the turbine. The boost converter on the other hand controls the electromagnetic torque of the generator. To boost the wind energy conversion efficiency of the system, the boost converter is coupled with a maximum power point tracking algorithm. At the grid side, the power inverter regulates the varying DC link voltage and controls the output power factor [6].

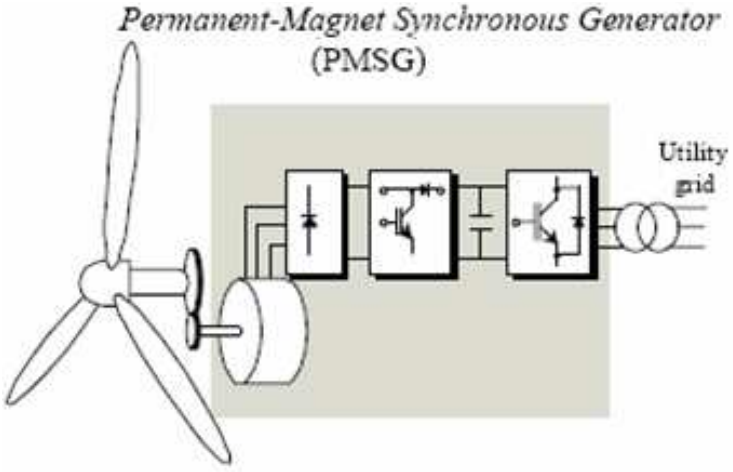

Figure 2.4: Common system setup with a permanent magnet wind turbine (generator is connected to the utility through a diode rectifier, boost converter and an inverter) [6]

.

The stator windings of the PMSG wind turbine in Figure 2.5 are connected to the

grid through two back-to-back PWM power converters. Maximum power point tracking algorithms are usually implemented in the utility side converter, but can generally implemented in either converter. The PWM modulation used in this configuration reduces the current harmonic component in the input and output of the system. By using PWM converters, there is also reduced torque pulsation on the generator and the output power quality is improved.

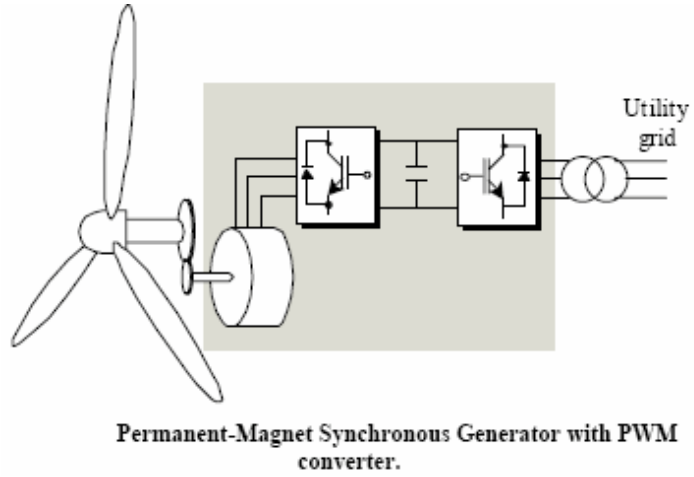

Figure 2.5: Common system setup with a permanent magnet wind turbine (generator is connected to the utility through two back-to-back converters) [6].

2.4.2 Induction Generators

Asides from synchronous generators, induction generators are widely used in wind turbines. A typical doubly fed wound rotor induction generator (DFIG) wind turbine configuration is illustrated by Figure 2.6. In the illustrated configuration, the stator is connected to the utility grid to provide the necessary magnetisation for the machine's operation. The rotor on the other hand, is connected to the grid through two

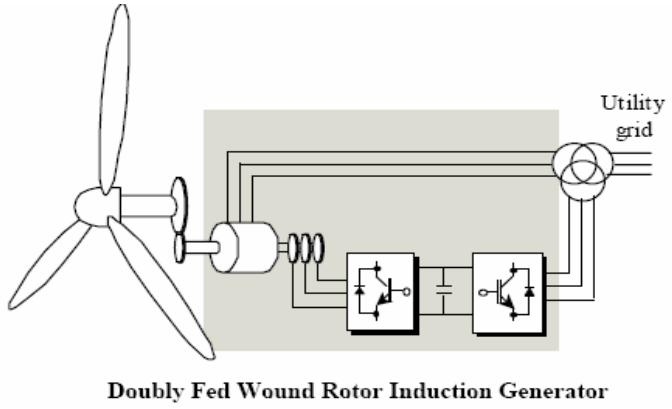

Figure 2.6: Common system setup with a doubly fed wound rotor induction wind turbine (the generator rotor is connected to the utility through two back-to-back converters, and the stator is connected directly to the utility)[6].

back-to-back PWM power converters. The rotor side converter regulates the electromagnetic torque and supplies some of the reactive power. To enable regulation of the electromagnetic torque, algorithms for extracting maximum power are implemented in the rotor side converter stage. The controller of the utility side converter regulates the voltage across the DC link for power transmission to the gird. There are reduced inverter costs associated with the DFIG wind turbine because the power converters only need to control the slip power of the rotor. Another advantage of the DFIG is its two degrees of freedom; the power flow can be regulated between the two wind systems (rotor and stator) [21]. This feature allows minimization of losses associated with a given operating point as well as other performance enhancements [21]. A disadvantage for using the DFIG wind turbine, however, is that the generator uses slip rings. Since slip rings must be replaced periodically, and so the use of DFIGs translates to more frequent maintenance issues and long term costs than other brushless generators. [6]

The stator of the squirrel cage induction generator (SCIG) in Figure 2.7 is connected to the grid through two back-to-back PWM converters. The stator side converter regulates the electromagnetic torque and supplies the necessary reactive power to magnetize the machine. The grid side converter on the other hand controls the power quality generated power to the grid. It accomplishes this task by regulating the real and reactive power delivered to the grid while regulating the (direct current) DC link voltage. The squirrel cage induction machine is very rugged, brushless, reliable, and cost effective. However, the drawback of using the SCIG is that the stator side converter must be oversized by 30-50% of machine's rated power in order to be able to satisfy the machine's magnetizing requirement. Therefore, although the SCIG itself is cost effective, the necessary power converters for its control are relatively more bulky and expensive. [6]

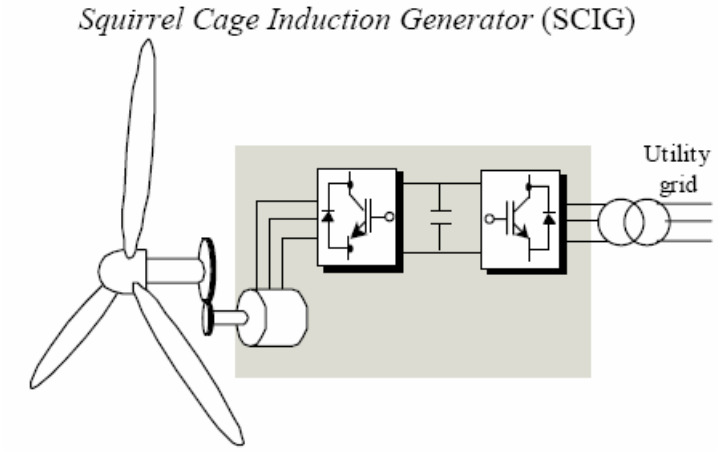

Figure 2.7: Common system setup with a squirrel cage induction generator (generator is connected to the utility through two back-to-back converters) [6].

2.5 Literature Review of Maximum Power Extraction Techniques

Since wind availability is sporadic and unpredictable, it is desirable to develop fast and efficient methods to track the optimal operation points of a variable speed wind energy system (WES). Many methods have been proposed and discussed in literature [13][7], [17][22][23]. This section will discuss methods that pertain to variable speed wind energy systems that use the PMSG generator.

The methods in [13] are based on the principle of loading the wind turbine to ensure that the maximum available energy from the wind is extracted. The two methods in [13] utilize the turbine characteristics (torque, power and power coefficient curves) to determine the operating point that results in maximum power capture. The only difference between the two methods presented in [13] is that one requires an anemometer so that the wind speed is physically measured while and the second method calculates the wind speed using electrical parameters. These methods are advantageous for fast optimum point determination and easy implementation since all the physical characteristics of the turbine are programmed directly and optimum operation point is determined by simply examining the characteristics. A disadvantage of these strategies however, is that they are customized for a particular turbine. In another words, if these strategies are to be used, they will need to be programmed with the turbine characteristics for the particular turbine in question. Another drawback of this algorithm is that it cannot take into account the atmospheric changes in air density, since for all its calculations, it assumes a certain value. The air density plays a significant part in the aerodynamics of the turbine, and thus affects the

accuracy of the pre-programmed turbine characteristics.

A maximum power point algorithm is proposed in [23] uses a maximum-efficiency control and a maximum-torque control to maximize the turbine output power. Based on the turbine characteristics of a selected turbine, the relationship between the optimum generator torque and the generator speed is established. This relationship determines the behaviour of the maximum-torque control. For any particular wind speed the generator torque balances the mechanical torque so that they will be equivalent at the optimum operating point. Since the generator torque is controlled in such a way that it tracks the optimum torque curve. An advantage of this method is that it does not require a wind speed detector. A drawback of this method is that to select the proportional constant that describes the relationship between the generator torque and speed is based on the turbine characteristics. This dependency hinders its ability to be used for various wind turbines, since different turbines have different characteristics.

The method in [7] is an Advanced Hill Climb Search (AHCS) that maximizes the power by detecting the inverter output power (P_{out}) and the inverter dc-link voltage. In their wind energy conversion system, they use a diode rectifier to first convert the three-phase output ac voltage from the generator to a dc voltage (V_{dc}). V_{dc} is related to the generator angular rotational speed (ω) by the generator field current (I_f) and the load current (I_g) of the PMSG: $V_{dc} = k(I_f, I_g) * \omega$ [7]. The authors in [7] noted that if the sampling period of the control system is adequately small then the term k(I_f, I_g) can be considered constant. The algorithm uses the relationship between the turbine mechanical power P_m, and the electrical system output power (P_{out}) given by (2.1). By differentiating (2.1) to get a relationship for ΔP_m, equation 2.2 is obtained.

$$P_m = P_{Load} + T_f * \omega + \omega * J\frac{d\omega}{dt} = \frac{1}{\nu}P_{out} + T_f * \omega + \omega * J\frac{d\omega}{dt} \tag{2.1}$$

$$\Delta P_m = \frac{1}{\nu}\Delta P_{out} + T_f * \Delta\omega + \Delta(\omega * J\frac{d\omega}{dt}) \tag{2.2}$$

In order to establish rules to adjust the system's operating point, this method evaluates the values of ΔP_{out} and $\Delta(V_{dc} * dV_{dc}/dt)$ (which represents $\Delta(\omega * d\omega/dt)$) based on (2.2). Depending on the values of ΔP_{out} and $\Delta(V_{dc} * dV_{dc}/dt)$ the polarity of the inverter current demand control signal (I_{dm}) is decided. There are three basic modes for this method, i) initial mode, ii) training mode, and iii) application mode. During its initial mode, before the algorithm has been trained, the magnitude of I_{dm} is determined by the max-power error driven (MPED) control. MPED control is the implementation of the conventional hill climb search (HCS) method in terms of wind energy system characteristics. During its training mode, the algorithm continually records and updates operating parameters into its programmable lookup table for its intelligent memory feature. Since this method is trainable with its intelligent memory, it allows itself to adapt to a turbine. As a result, it is a solution to the customization problems of many algorithms. Another advantage of this algorithm is that does not require mechanical sensors (like anemometers) which lowers its cost and eliminates its associated practical issues. However, it can be seen in [7] that the algorithm is relatively slow and complex as it has three different modes of operation. Another drawback is that the algorithm cannot take into account of the changes in air density, which affects the power characteristics quite significantly [17] (see Figure 2.8). Its lookup table updating process will be adversely affected due fluctuations in air density. The updating method in [7] states that the lookup table, which constitutes

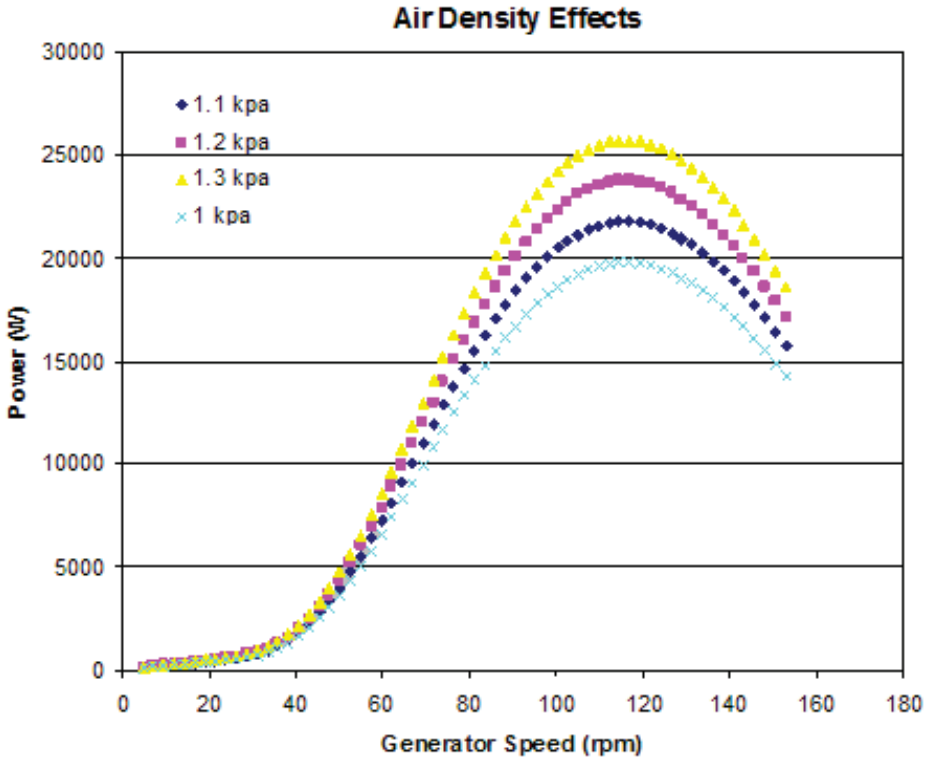

Figure 2.8: Affects of air density on the power extracted from the wind at 9 m/s.

V_{dc}	P_{dm}	I_{dm}
76	0	70
101	64.8	70
126	226	66.6
151	390.4	60.8
176	619.9	58.2
201	926.9	53.1
226	1317.4	47.1
251	1808.5	47.6
276	2409	44.2
301	3124.1	39.7
326	3976.4	31.9
351	4966	28.6
376	6110.4	35.9
401	7415.6	43.6
426	8894.8	52.3
451	10558.4	62.1
476	11775.3	69.2
501	11902.4	70
550	12000	70

(a)

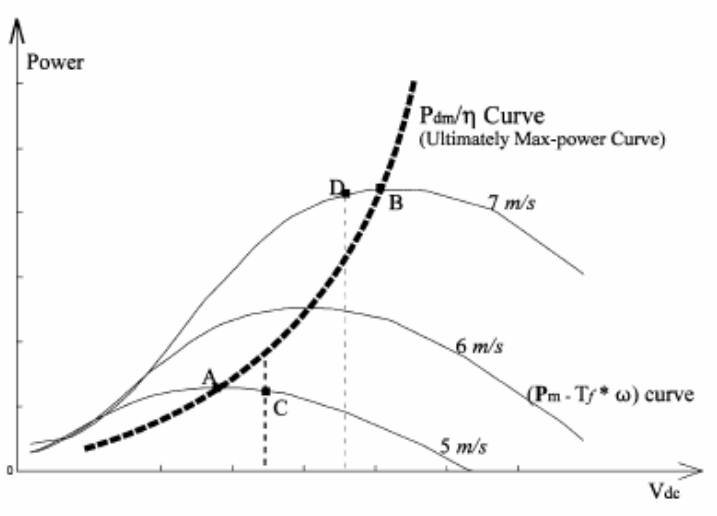

(b)

Figure 2.9: a)Intelligent Memory Lookup Table ; b)Power characteristic of turbine with respect to V_{dc}[7].

as its intelligent memory feature, is updated when three particular conditions are met. The conditions are i) that the system is in steady state (wind speed is stable), ii) that the system is operating in the down-hill region of the power curve, and iii) that the current output power (P_{out}) is greater than the recorded demanded output power (P_{dm}) for a particular V_{dc}. Figure 2.9a) is an example of the intelligent memory lookup table used in [7]. Figure 2.9b) is the power characteristic of the turbine where a particular V_{dc} is generated by the generator corresponds to a particular generator speed. If the measured P_{out}, providing that conditions i), ii) and iii) are met, is greater than the P_{dm} that corresponds to the V_{dc} nearest to the current V_{dc}, then the compared entry is replaced with the new V_{dc}, $Pout$ and I_{dm} (current demanded that provides the new P_{out}) values. If the air density is constant then the algorithm can effectively determine the max-power curve as shown in Figure 2.9b).

However, with changing air densities, it can be seen that the Max-power curve

shifts with a change in air density as shown in Figure 2.10. With the updating rules in [7], the highest P_{out} value for a particular V_{dc} in the downhill region of the power curve represents the maximum power point. Ultimately, the max-power curve will be for the highest air density and thus inaccurate for lower air density conditions.

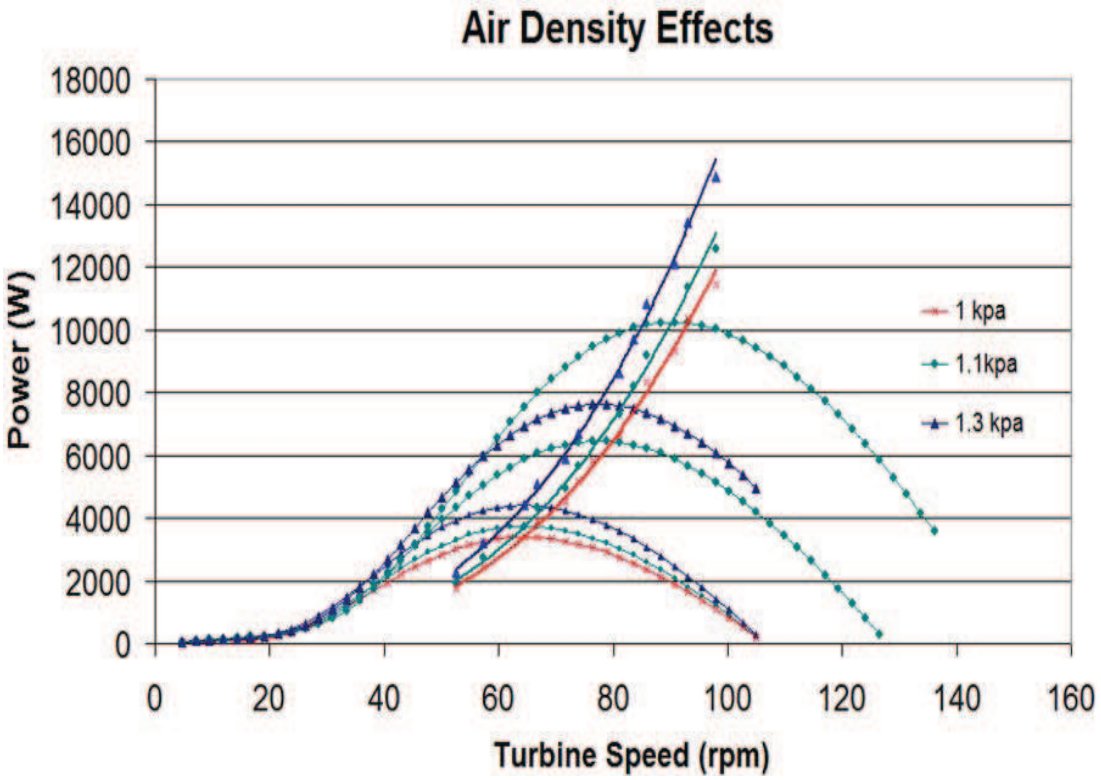

Figure 2.10: Maximum Power curves for different air densities.

In [17], the wind turbine is connected to a battery through a rectifier, and a DC/DC converter. The proposed MPPT algorithm adjusts the operation point of the wind conversion system by directly adjusting the DC/DC converter duty cycle based on the comparisons of the output power measurements. The basis of the algorithm is very similar to the Hill Climb Search (HCS) method as proposed by [7], [22]. The distinctive feature is that the adjustments are implemented through a relationship

found between the change in output power and the duty ratio. Relationships between the duty ratios of the buck, buck-boost, and boost converters and the change in output power have been described in [17]. Thus, the algorithm determines the operation point adjustment based on the change in power with respect to the duty cycle.

The proposed algorithm in [22] searches for the peak power by changing the speed reference in the appropriate direction. Depending on the magnitude and direction of change in active power, the speed reference is modified towards it optimal operating point. The peak power points are identified on the power versus generator shaft speed curve where its derivative is zero; the power curve looks similar to that of an inverse parabola see Figure 1.7.

In [22], the output power and speed are sampled at regular intervals of time, and if the wind velocity is stable and the system was originally at its optimum point, then no action is taking. When there is a step change in wind velocity, the turbine is no longer operating at its optimum point and there will be a corresponding change in power. Positive power change corresponds to increased speed reference proportional the change in power, and a negative power change corresponds to decreased speed reference. For further adjustment (when wind speed is stable) the speed reference direction is determined by both the change in power and the previous speed reference direction. For example, if a reduced speed reference resulted in a positive change in power then the system will continue reduce the speed reference. When the change in power is minimal (within a predefined limit) then no further change in the speed reference is made (since the minimal change in power translates to the peak power point). A disadvantage of this algorithm is that uses the turbine characteristics (torque, power and power coefficient curves) to determine the amount of change in

the speed reference with respect to the change in power. This introduces dependence of the algorithm to the characteristics of a particular turbine. Another drawback of this algorithm is that it does not have any means to store the previously determined peak power operating points. This means that with each change in wind speed, the algorithm will have to search for the optimum point even if it has been previously determined. The repetitiveness of the searching procedure will slow down the optimum point determination process and cause subsequent losses potential output power.

2.5.1 Summary of MPPT Algorithms

The methods in [7], [17], [22] use the changes in power (ΔP) and the changes in generator speed ($\Delta\omega$) to adjust the generator speed towards the optimum operating point. The intelligent memory in [7] allows the algorithm to be more efficient over time as the optimal points are stored, when determined, for later use. The methods in [7],[17], [22] are independent of turbine characteristics, so they are flexible and can be applied to various turbines. These algorithms, however, would be slower than those in [13] and [23] because of their adjustment process. The algorithms described in [13] and [23] fast and efficient, but they are dependent on having prior knowledge of the turbine characteristics. Therefore the methods in [13] and [23] cannot be used for a wide range of turbines and cannot consider machine degradation since they cannot adapt to change.

Chapter 3

Proposed Algorithm

3.1 Algorithm Concept and Features

The proposed algorithm uses the HCS methodology along with intelligent memory and power management to track the maximum power points of wind energy systems under fluctuating wind conditions. The main problems in existing power extraction methods are: i) customization, ii) speed, and iii) wasted power. The proposed algorithm provides a solution to these problems. In order to avoid the customization problems in some of the existing algorithms, the proposed technique does not require the characteristics of the turbine to be preprogrammed. Instead, the algorithm initially uses a general estimate of the turbine characteristics and then determines the actual characteristics through operation. By doing this, the algorithm can be easily used for a wide range of wind turbines. The turbine adaptation feature of the algorithm allows it to immediately make fairly accurate estimations on the maximum power points of the system following the determinations of the maximum power

points. The estimations allow the system to immediately operate near to the maximum power point, where the change in speed corresponds to small changes in power. Therefore, the estimations lead to less wasted potential power and speed up the determination process. The closer the operating point is to the maximum power point, the fewer adjustments necessary.

The proposed algorithm has two main concepts to enable flexible, fast and efficient maximum power extraction. The first concept is to quickly determine the maximum power point by using the turbine fundamental tip-speed ratio equation in conjunction with the HCS methodology. The second concept is to enable immediate maximum point retrieval for reoccurring wind speeds and determination of the given turbine's internal actual TSR. Recall that the TSR is the ratio of the wind speed and the rotor speed, and for each turbine there is one TSR that will always result in maximum power transfer. The TSR is characterizes the aerodynamic efficiency of a wind turbine and is unique. Please note that the dynamic response of the generator dictates the speed at which the algorithm can determine an optimum point. This is because the system will not make any decisions or adjustment to the speed reference until it has reached steady-state (i.e. reached the reference for a defined period of time).

3.1.1 Modified Hill Climb Search

Due to the nature of wind energy systems described in chapter 1, the power available from the wind turbine is a function of both the wind speed and the rotor angular speed. The wind speed being uncontrollable, the only way to alter the operating point is to control the rotor speed. Rotor speed control can be achieved by using power electronics to control the loading of the generator. Without any given knowledge of

the aerodynamics of any wind turbine, the HCS principle searches for the maximum power point by adjusting the operating point and observing the corresponding change in the output. The HCS concept is essentially an "observe and perturb" concept used to traverse the natural power curve of the turbine. With respect to wind energy systems, it monitors the changes in the output power of the turbine and rotor speed. The maximum power point is defined by the power curve in Fig. 3.1 where $\Delta P/\Delta\omega = 0$. Thus, the objective of HCS is to 'climb' the curve by changing the rotor angular speed and measuring the output power until the condition of $\Delta P/\Delta\omega = 0$ is met. There are several different ways of implementing the HCS idea.

In this thesis, the algorithm generates the reference speed by measuring the output power of the wind energy conversion system and adjusts the system's operating point accordingly. The $\Delta P/\Delta\omega = 0$ condition is achieved when $\Delta P \approx 0$ because the amount of adjustment in the rotor speed is chosen to be proportional to the change in power; thus when $\frac{\Delta P}{\Delta\omega} \approx 0$. The HCS concept is described in detail in this section according to this thesis' implementation method and it is illustrated by Figure 3.1.

The system begins at point 1 and chooses to increase the rotor speed to point 2. Observing that that there has been an increase in power due to an increase in speed, the algorithm signals to further increase the rotor speed to point 3. Since $\Delta P/\Delta\omega$ is positive, the system is 'climbing' up the power curve. With $\Delta P/\Delta\omega$ still positive, the system continues to increase the rotor speed to point 5. The algorithm notices that the change in power from point 4 and point 5 is negative, and it was due to an increase in speed. With $\Delta P/\Delta\omega$ now negative, the optimum point has been passed. As a result, the rotor speed is decreased to point 6. The slope of the power curve diminishes as the system approaches the peak power point (level of extracted power

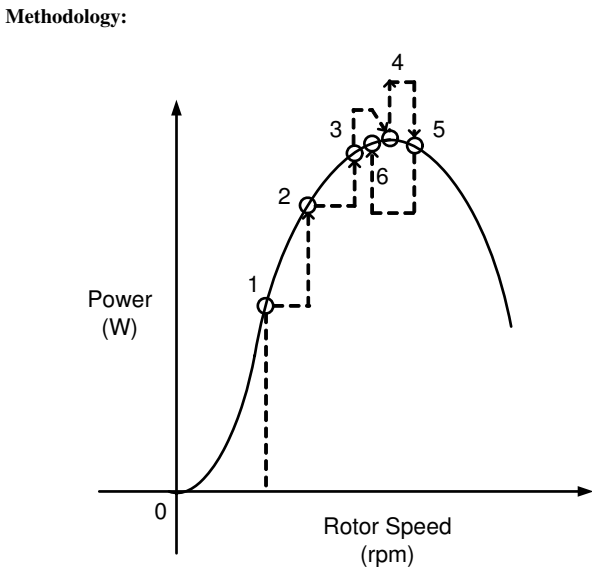

Figure 3.1: Wind power curve for an arbitrary wind speed. This figure illustrates the concept of the "observe and perturb" of HCS.

is less sensitive to the change in rotor speed, $\frac{\Delta P}{\Delta \omega} \rightarrow 0$). Therefore, it follows that as the operating point moves closer to the maximum power point (point (4)), the magnitude of the speed adjustment should be smaller. The algorithm will oscillate and eventually settle at the maximum power point (which is defined to be where $\Delta P/\Delta\omega = 0$).

3.1.2 Adaptive Memory

HCS gives the algorithm the ability to search for the maximum power point, but by also using the TSR relationship and memory, the search process is sped up considerably. An anemometer provides the algorithm with the knowledge of the wind conditions so that the system can quickly respond with the correct decisions. For each turbine, the operating points at which the maximum power is attained is defined by

the wind speed and its corresponding rotor speed. In order to keep the system independent from the physical characteristics of the wind turbine, and thus keeping it easily modifiable to other turbines, an approximate "optimal" TSR is used initially.

The memory feature of this algorithm not only allows immediate access to the maximum power points previously determined, it also enables the algorithm to adapt to its given turbine. The adaptability of the algorithm allows the system to capture as much available power as possible under fast wind variations. The memory provides two major power management functions; i) store the operating points as determined by the algorithm, ii) to update the approximate TSR to a value nearer to the actual TSR.

The algorithm stores the determined operating points with respect to the wind speed. This allows the system to immediately jump to the optimal operating point, thereby bypassing the time-consuming searching procedure. In the case that the stored operating point is not ideal, after the determined maximum power point is reached, small adjustments are made to ensure the integrity of the stored data. With small adjustments, minimal power is wasted during this process because the system will be operating very close to its maximum efficiency.

With each successful determination of a maximum power point, the data is used to obtain a more accurate TSR using (1.5). Since it is known that the maximum power point for a particular turbine always occurs at the same optimal TSR for all wind speeds, the TSR is updated to be the average TSR obtained from each data entry. As a result, each time a new wind speed occurs, the approximate operating point, using the updated TSR, will become closer and closer to the actual maximum power point. Thus, the searching process is continuously shortened with each optimum point

determination.

3.1.3 Algorithm Structure

Figure 3.2, 3.3, and 3.4, illustrate the different stages of the proposed algorithm logic. It is necessary to note that all measurements and adjustments are made after the system is steady at its current operating point. This prevents incorrect decision due to transient fluctuations.

Figure 3.2 illustrates the algorithm in its initial state. When the algorithm begins, the rotor speed reference is calculated using the given the wind speed (from the anemometer) and the initial TSR. The rotor speed reference is then applied to the wind energy conversion system (WECS). After system has reached the specified reference speed, a measurement of the WECS output power is taken.

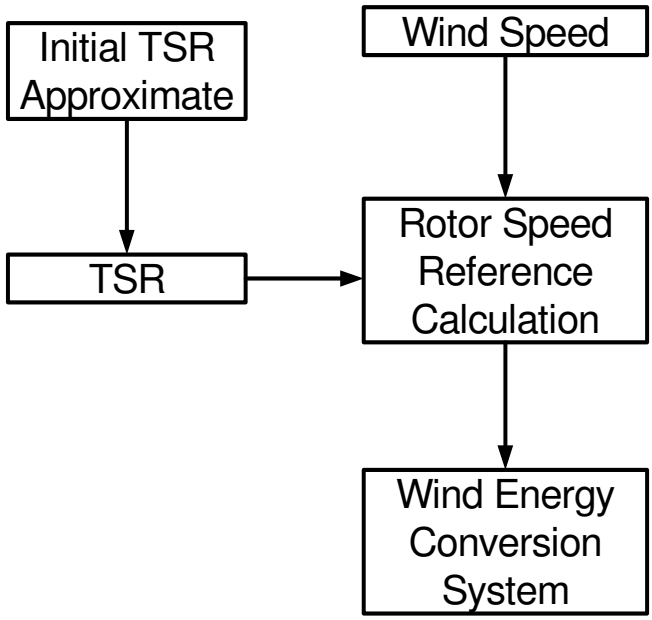

Figure 3.2: Illustration of proposed algorithm logic at the initial stage.

If the wind speed is constant, then the algorithm will proceed to its second state, illustrated by Figure 3.3.

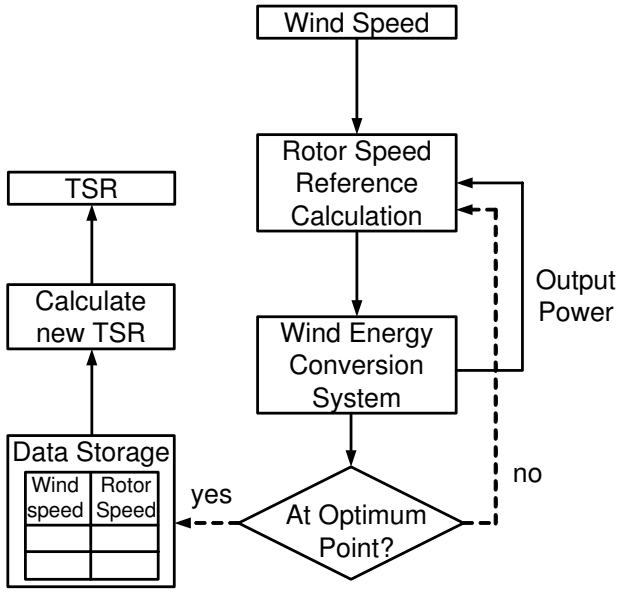

Figure 3.3: Illustration of proposed algorithm logic in the second stage (after initial startup and when there is no change in wind speed).

With the wind speed constant, the output power measured from the WECS and the algorithm determines the difference between the current power and the previously measured output power. This information is used in the algorithm's modified HCS segment. When an optimum point is found, it is stored in memory. With the updated memory, an updated value for the TSR is calculated for later use.

The new TSR is used instead of the initial TSR because it is calculated based on the actual turbine rather than just an approximate. When faced with wind speeds that have not yet been recorded, the use of the calculated TSR leads to more accurate approximations of the turbine optimum speed. With more accurate approximations, less adjustment towards the optimum point is necessary and therefore the search

process is further sped up.

Figure 3.4 illustrates the algorithm when there is a significant change in wind speed. If the wind speed has been previously recorded, the algorithm will apply the stored optimum rotor speed to the system. Otherwise, the algorithm will calculate an approximate optimum rotor speed using the wind speed and either the initial or calculated TSR. Providing the wind speed has not changed, the algorithm will then go back to the operation stage illustrated by Figure 3.3.

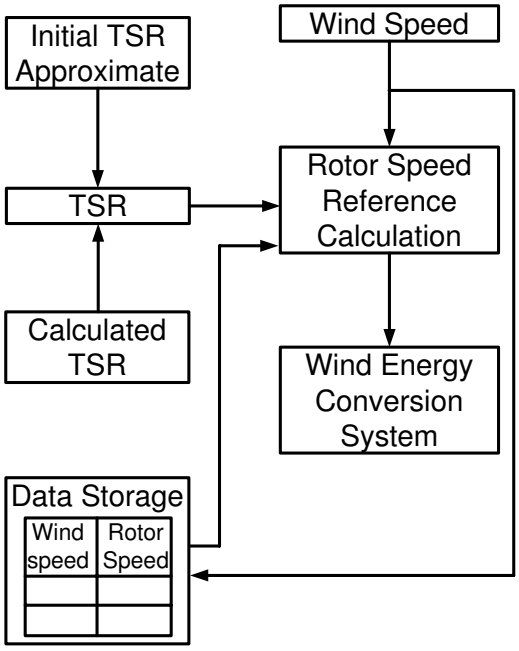

Figure 3.4: illustration of algorithm in the even of a wind speed change.

3.2 Algorithm Implementation

In order to accomplish the tasks described in the algorithm concept section, the proposed MPPT algorithm is comprised of two loops: i) a change detecting loop

(CDL) and ii) an operating point adjusting loop (OPAL), (See Figure 3.5). The algorithm's adaptive and optimum point search feature is achieved by a programmable array and a programmable lookup table that are trained by OPAL and used by CDL. The modified HCS is realized with both the CDL and OPAL working together.

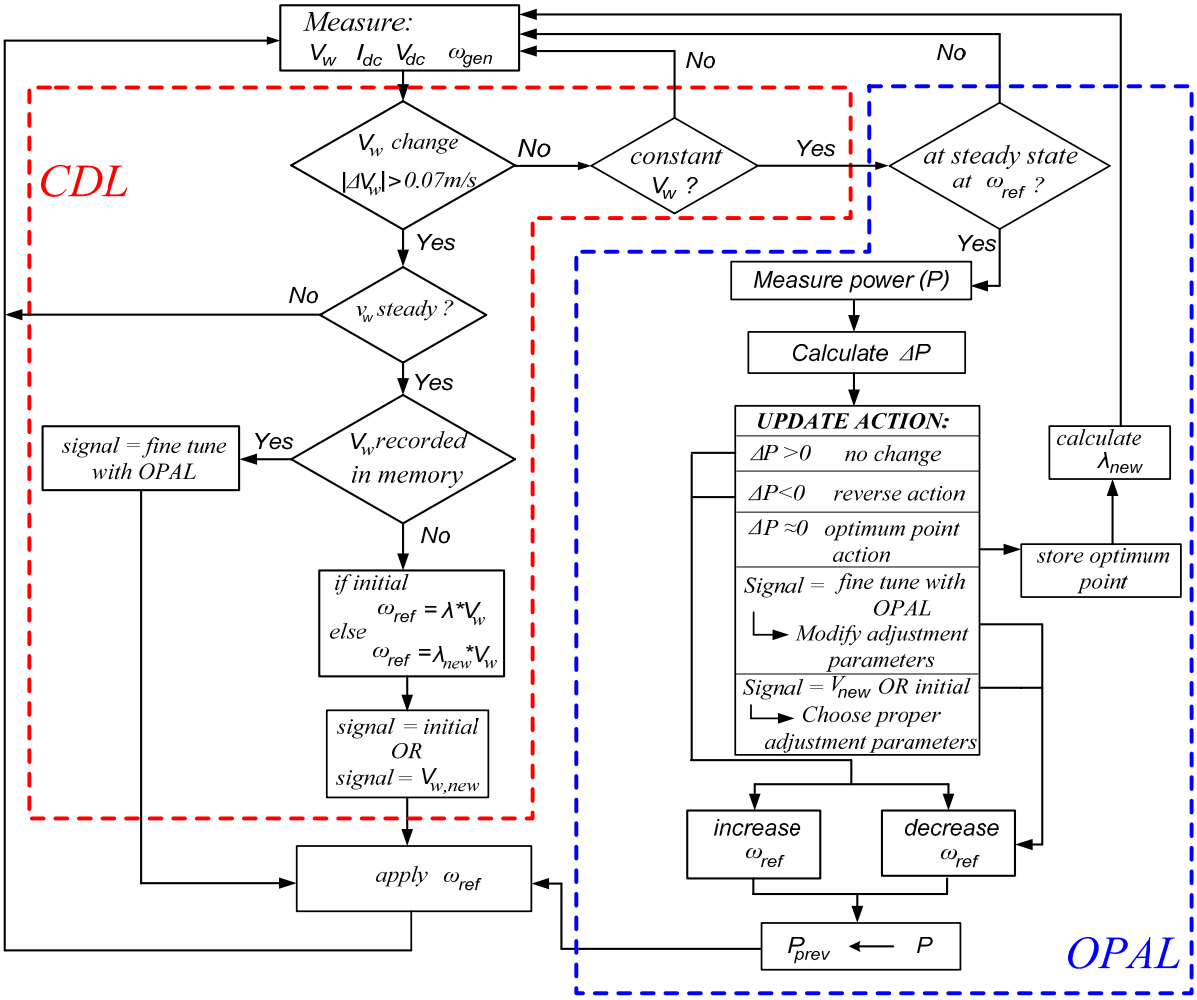

Figure 3.5: Logic Flow of the proposed algorithm.

A. Change Detection Loop (CDL)

The CDL is a fast detection loop that continually monitors the wind conditions

and executes the actions necessary to efficiently determine the optimum point while minimizing the loss of potential wind energy. Whenever the system is not operating at its ideal operating point for a particular wind velocity, the amount of potential wind energy lost can be quite significant. Therefore, the speed of the CDL is crucial to manage the algorithm so that incorrect decisions due to the fluctuations in the wind can be immediately corrected. CDL is executed initially and whenever a change in wind speed is detected. When a wind speed change has been detected, then it will initiate the execution of OPAL, determine an approximate maximum power point, or search for a previously recorded optimum power point.

Upon startup, the algorithm calculates an initial reference speed, ω_{ref}, by using (1.3), where $\lambda = 7$. This value of the tip-speed ratio is a generic λ_{opt} for a 3-blade wind turbine as suggested by [24]. The selected initial value for the TSR is not optimal, so the calculated speed reference will not be the optimal point. However, by using the suggested value of an optimal TSR for a generic turbine, it allows the system to begin at an operating point near the actual maximum power point rather than at an arbitrary point.

The algorithm is programmed in C++ through the power simulator program (PSIM). Since wind is always constantly fluctuating, a wind speed is considered steady when the changes are within ± 0.07 m/s (0.252 km/h). To detect this, the fast CDL loop measures the current wind speed, $v_w(n)$, and compares to the previous stored value, $v_w(n-1)$. If the difference, v_w, is within the specified range to be considered constant for a specified amount of time, then no further action is taken by CDL and OPAL will be executed. However, if $\mid v_w \mid$ is greater than the specified threshold, CDL will search through the lookup table (programmed by OPAL) to see if the current

wind speed is within ±0.07 m/s of any recorded wind speed.

If a stored wind speed within ±0.07 m/s of the current wind speed is found, then the corresponding recorded ω_{opt} is used as the reference speed and OPAL will be signaled to make minor adjustments to ensure the integrity of the stored data. Since each optimum point is determined through operation it may not be the exact optimum power point, instead it will be an operating point that is extremely close to the maximum power point. To further move the operating point closer to the actual maximum power point rather than deviating, small adjustments are made to ensure that the applied speed reference is the maximum point. In the case that it is not as optimal, the small adjustments will fine tune the stored maximum operating point to its true value. Due to the flat-topped nature of wind power curves, small adjustments around the maximum power point will not result in much loss of potential wind power. The immediate use of a stored optimal speed allows the algorithm to eliminate any redundant searches that have been done before. Standard HCS will always go through the full search each time the wind speed changes and causes it to be slower and therefore more potential energy is wasted.

In the case that the current wind speed is not within ±0.07m/s of any stored wind speed in the database, then ω_{ref} is calculated with either the updated λ_{new} (determined by OPAL) or the initial λ, and OPAL will be signaled to be executed to adjust ω_{ref} towards the optimum point.

B. Operation Point Adjusting Loop (OPAL)

This process is executed when it is signaled by CDL. Its main task is to adjust the system's operating point towards the optimum generator speed, ω_{opt}, using a modified hill climb search (HCS) method and to train the adaptive memory.

OPAL determines whether the generator should be sped up or slowed down depending on ΔP, system status, and the change in speed reference based on a modified HCS principle (See Table 1 for the modified HCS decision parameters). Thus, depending on the decision parameters, ω_{ref} is adjusted accordingly towards ω_{opt}. To avoid unnecessary computations that cause the system to take a longer time to find the optimum point (due to incorrect decisions), no adjustment to ω_{ref} is made until the system has reached steady state at the current ω_{ref}.

The adaptive feature is realized by a programmable look up table and a programmable array that are trained by updating it whenever a ω_{opt} is determined for a new wind speed. The look up table is updated by storing the determined ω_{opt} and its corresponding wind speed into memory. The array, on the other hand, is updated by storing the calculated λ_{opt} from the ω_{opt} and wind speed values. The average of the recorded λ values in the array then becomes λ_{new} (an approximate of the actual λ_{opt}) for the next CDL iteration. The optimum point determination process is sped up by the adaptive feature as the look up table allows the system to immediately obtain the ω_{opt} for a reoccurring wind speed. The array also speeds up the process by allowing the CDL to obtain a fairly accurate ω_{ref} so that minimal adjustment by OPAL is required.

B.1 Modified Hill Climb Search

The concept behind the modified HCS method is to determine the power change (ΔP) with respect to the change in rotor speed while using the TSR and memory to jump to an operating point closer to the maximum power point. Unlike the standard HCS method, the proposed algorithm's TSR concept and memory guarantees the system to immediately begin at a point relatively close the maximum power point

rather than at an arbitrary point. Due to the shape of the power curve, this 'jumping' feature of the algorithm limits the amount of wasted potential power. Figure 3.6 illustrates the algorithm where the search procedure is the combination of the HCS and the TSR.

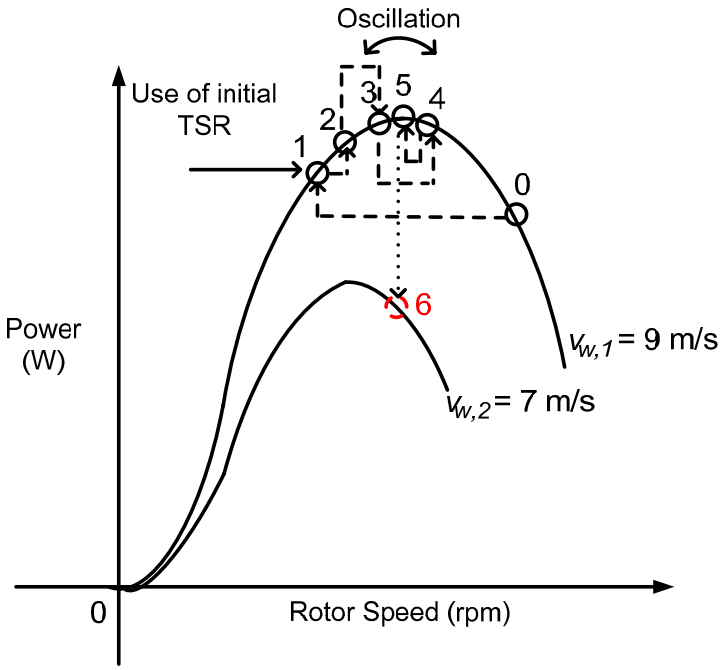

Figure 3.6: Illustration of the proposed algorithm's adjustment process (startup).

As illustrated by Figure 3.6, the system reacts to the wind speed of 9 m/s and begins at an arbitrary point (point 0). With the knowledge of the wind speed and the initial generic TSR value, the approximate maximum power point (point 1) is determined. Once the system has settled at the specified approximate power point, the power measured and stored as "current power". The system is considered to have settled at an operating point when it has reached the reference speed for a specified period of time. This is done to ensure that no measurements or decisions are made until the system is has indeed reached the reference point.

Since it is during the initial startup of the algorithm, the algorithm has no knowledge of any maximum power points, the turbine's optimum TSR, or where the current operating point lies on the power curve. As a result, the algorithm has two choices. It can arbitrarily choose to either increase or decrease the current generator speed by 3% and observe the effects. Here, the proposed algorithm is programmed to initially increase the rotor speed. Once the reference speed (97% of the current rotor speed) is applied to the system, the algorithm monitors the system response. Once the algorithm detects that the system has settled at the specified speed (point 2), the power is measured. The previously measured power at point 1 is stored now as "previous power" and the new measurement at point 2 replaces the "current power". Noticing an increase in power from point 1 to 2 as a result of the increase in rotor speed, the algorithm continues to increase the rotor speed. Now, with data regarding the increase in power as a result of the change in speed, the speed reference is increased by half of the change in power, ΔP (where ΔP = current power - previous power). In addition, because both $\Delta\omega$ and ΔP are positive, the algorithm acknowledges that it is currently operating at a point that is to the left of the maximum power point. This process continues until the system reaches point 4. From point 3 to 4, there is a decrease in power corresponding to the increase in speed, so the algorithm acknowledges that the optimum power point has been passed. Consequentially, the algorithm decreases the rotor speed proportionally to the change in power and the system. Whenever the algorithm detects a negative change in speed, the speed reference change will reverse in direction. As a result, the system will oscillate around and eventually settle at the optimum point (point 5). As illustrated in Figure 3.6, because of the gradual decrease in the change in power, as the operating point becomes nearer and nearer to

the maximum power point, the change in rotor speed also decreases. When the ΔP is detected to be within $\pm 0.5\%$ of the current power, then it is considered to be almost zero. However, if 0.5% of the current power is more than 30W, then the specified range where ΔP is considered zero is limited to 30W. Since $\Delta\omega$ is proportional to ΔP, the maximum power point ($\Delta P/\Delta\omega = 0$) is reached when $\Delta P = \pm 0.5\%$ of the current power or ($\pm 30W$). Once the maximum power point has been reached, the wind speed and current speed is recorded into the memory. The data is then used to calculate the optimal TSR for the specified turbine to replace the initial generic TSR value.

Due to a change in wind to 7 m/s after the maximum power point has been determined for 9 m/s, the operating point shifts to point 6. Because of the inertial properties and the system's mechanical time constant, the system speed does not change immediately. As a result, the system will continue to operate at its previous speed, but the operating point is no longer optimal. Figure 3.7 illustrates the algorithm operation under a new wind condition after an operating point has been determined.

Once a new wind speed has been detected, CDL is invoked and a new speed reference is generated using the determined TSR value from the previous maximum power point. Since the optimum TSR for maximum power transfer for a turbine is the same under all wind conditions (since it is the ratio between the rotational speed and the wind speed), the determined TSR will be valid for the new wind speed. Therefore, the approximate optimum speed (point 8) will be very close to the actual maximum power point. Because the operating point is so close to the actual maximum power point, subsequent adjustments to the reference will be small to ensure that the

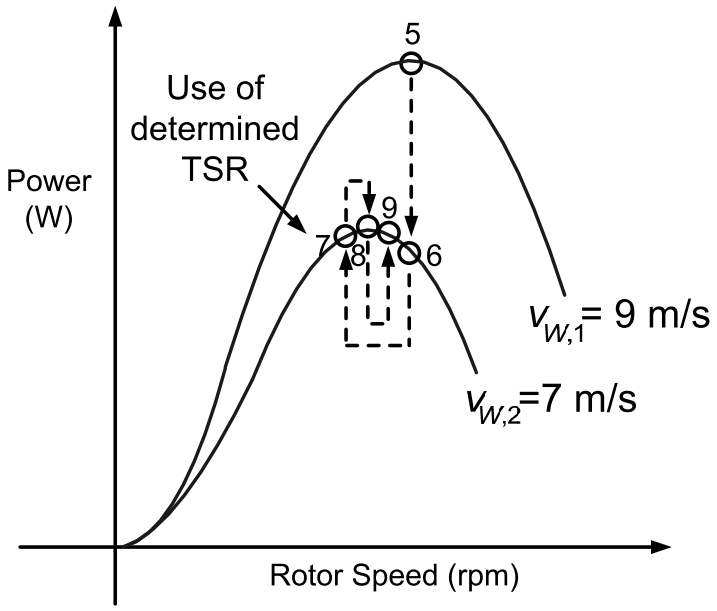

Figure 3.7: Illustration of the proposed algorithm's adjustment process (wind change after startup).

operation point will not stray too far away. However, the same adjusting principles discussed earlier are still used. As a result, the system will oscillate around and eventually settle at the maximum power point (point 9).

It is important to note that in order to take into the account of the relatively slow time constant of the system, the OPAL measurements and adjustments are always made after the system has reached the previously defined reference speed for a defined period of time. This is to avoid incorrect decisions in case of fluctuations around the reference speed (undershoots and overshoots) that may incorrectly confuse the algorithm that the system has reached the specified reference value.

Chapter 4

System Modelling

The main focus of this thesis is to provide a control algorithm for wind energy systems to extract as much power as possible from the wind, so the turbine-generator values were chosen based on [25] to emulate a wind energy system. The most important function of system modelling in this thesis is to ensure that the torque and power transfer from the wind turbine to the generator relationship is correct. It suffices to have the designed system to behave similarity to the WECS presented in literature. The system was also modelled in such a way that effects, such as tower shadow, etc., were neglected so that the system can reflect the performance of the control algorithm clearly.

The system considered in this thesis is a front-end rectifier system, where its main purpose is to rectify the generator output voltage and control the system to shift the system operating point to enable maximum power extraction. The WECS considered in this thesis is illustrated in Figure 4.1. The system consists of a wind turbine, permanent magnet synchronous machine, a diode rectifier, and a boost converter.

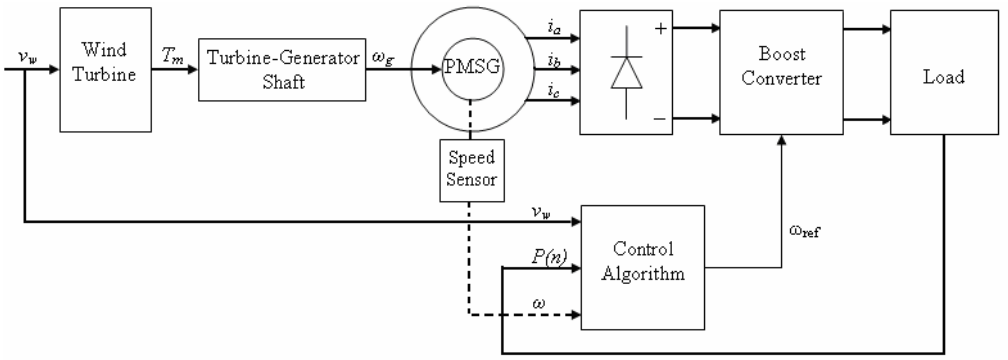

Figure 4.1: Wind energy conversion system block diagram.

4.1 Wind Turbine Modelling

Since the power coefficient characteristic a non-linear curve that reflects the aerodynamic behavior a wind turbine, this curve must be defined. The C_p curve in this thesis is taken from the wind turbine model provided by Matlab Simulink [26]. The characteristic forms the basis for the custom turbine model. The non-linear, dimensionless C_p characteristic given by Simulink is represented by the (4.1) and (4.2) [26]:

$$C_p(\lambda, \beta) = c_1(\frac{c_2}{\lambda_i} - c_3\beta - c_4)e^{\frac{-c_5}{\lambda_i}} + c_6\lambda \tag{4.1}$$

$$\frac{1}{\lambda_i} = \frac{1}{\lambda + 0.08\beta} - \frac{0.035}{\beta^3 + 1} \tag{4.2}$$

Where $c_1 = 0.5176$, $c_2 = 116$, $c_3 = 0.4$, $c_4 = 5$, $c_5 = 21$, $c_6 = 0.0068$

Several modifications have been made to the Simulink wind turbine model. First, the wind turbine model was changed from a per unit system to a real value system in order to make the turbine model compatible with the real value components of the WECS. Second, the original model represents a variable pitch model, while for the purpose of this thesis the model was changed to represent a fixed pitch turbine. The fixed pitch model was used to isolate the effects of electrical control rather than

mechanical control because pitch control is achieved through hydraulic manipulation. Therefore the new power coefficient equation (4.3) is derived from the substitution of (4.2) into (4.1) and modifications:

$$c_p(\lambda) = 0.5176(\frac{116}{\lambda} - 116 * 0.035 - 5)e^{\frac{21}{\lambda} - 21*0.035} + 0.0068\lambda \tag{4.3}$$

This new power coefficient curve is illustrated in Figure 4.2.

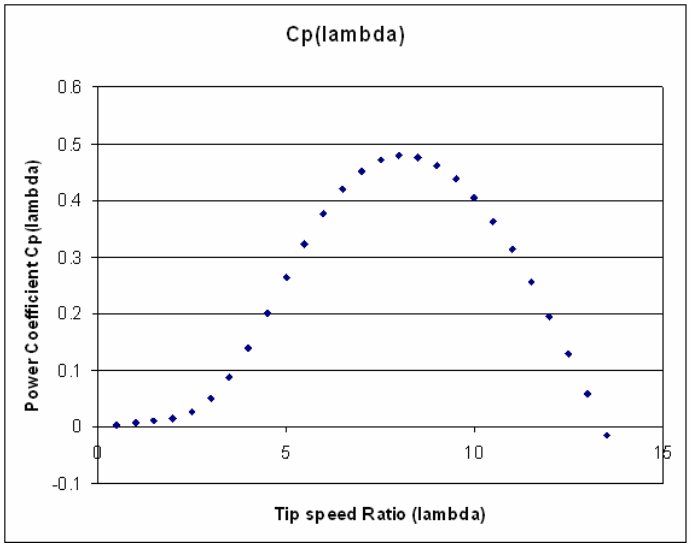

Figure 4.2: C_p Characteristic of Custom Wind Turbine Model.

The power and torque characteristics of a wind turbine are governed by equations (1.3) and (1.6). With the power coefficient function given by (4.3), the mechanical power of the turbine can now be represented by substituting (4.3) into (1.1), with $\beta = 0$, and substituting the coefficients to give:

$$p_m = 0.5\rho A(0.5176(\frac{116}{\lambda} - 116 * 0.035 - 5)e^{-(\frac{21}{\lambda} - 21*0.035)} + 0.0068\lambda)v_w^3 \tag{4.4}$$

The torque is defined by equation (1.3), where after substituting p_m it becomes:

$$t_m = 0.5\rho A(0.5176(\frac{116}{\lambda} - 116 * 0.035 - 5)e^{-(\frac{21}{\lambda} - 21*0.035)} + 0.0068\lambda)v_w^3 \frac{R}{G\lambda v_w} \tag{4.5}$$

Which, after λ is replaced by $\frac{\omega R}{v_w}$ from (1.2), (4.5) becomes:

$$t_m = 0.5\rho A(0.5176(\frac{116v_w}{\lambda R} - 116 * 0.035 - 5)e^{-(\frac{21v_w}{\omega R} - 21*0.035)} + 0.0068\frac{\omega R}{v_w})\frac{v_w^3}{G\lambda v_w} \quad (4.6)$$

The equations (4.4) and (4.5) represent an arbitrary turbine with the aerodynamic efficiency illustrated by Figure 4.2. The customized turbine model's specifications are summarized by Table 4.1 and the theoretical power and torque characteristics of a wind turbine are illustrated by Figure 4.3 and 4.4.

Table 4.1: Customized wind turbine parameters

Number of blades	3
Blade radius	6 meters
Gear ratio	30
Pitch	Fixed Pitch

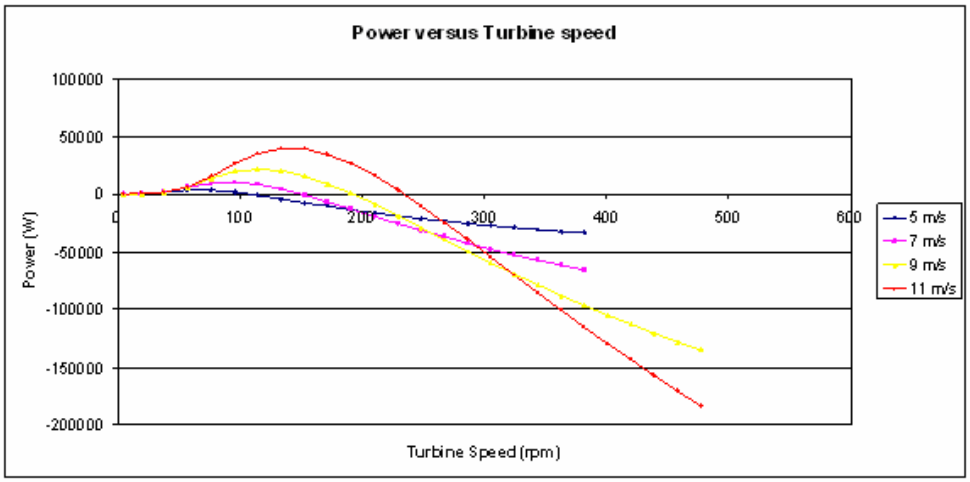

Figure 4.3: Output Mechanical Power of Turbine versus the Turbine Speed (Air density: 1.1 kpa).

Figure 4.5 is the wind turbine model built in Simulink by implementing the equations specified by (4.3) - (4.5). Since the power coefficient varies with the tip speed ratio, a gradual increase generator speed (represented by a ramp function) and a

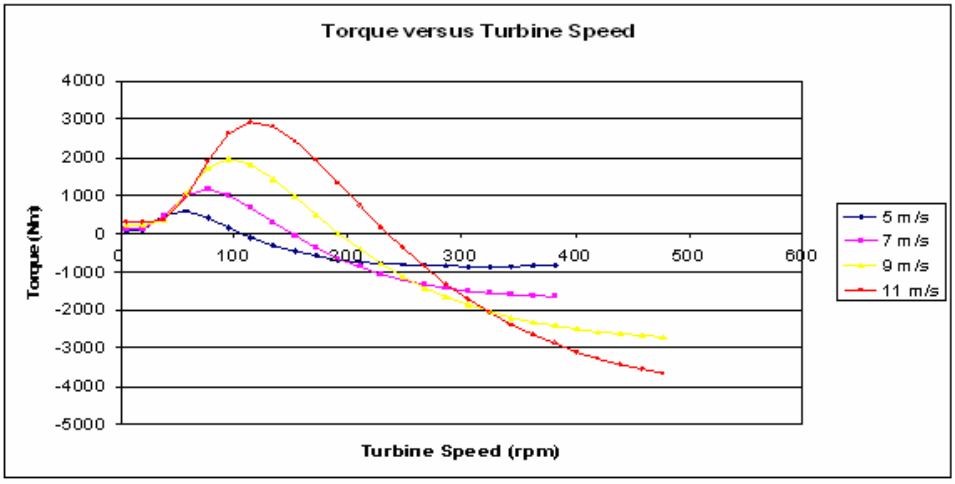

Figure 4.4: Output Mechanical Torque of Turbine versus the Turbine Speed (Air density:1.1 kpa)

fixed wind speed was applied to compare the simulated turbine C_p curve with the theoretical C_p curve. (See Figure 4.6)

With the main focus of the shaft modelling on the correctness of the torque and speed transfer to the generator, the main relationship between the turbine output torque and the generator rotor speed is given by (4.7).

$$T_m = J_s \frac{d\omega}{dt} \tag{4.7}$$

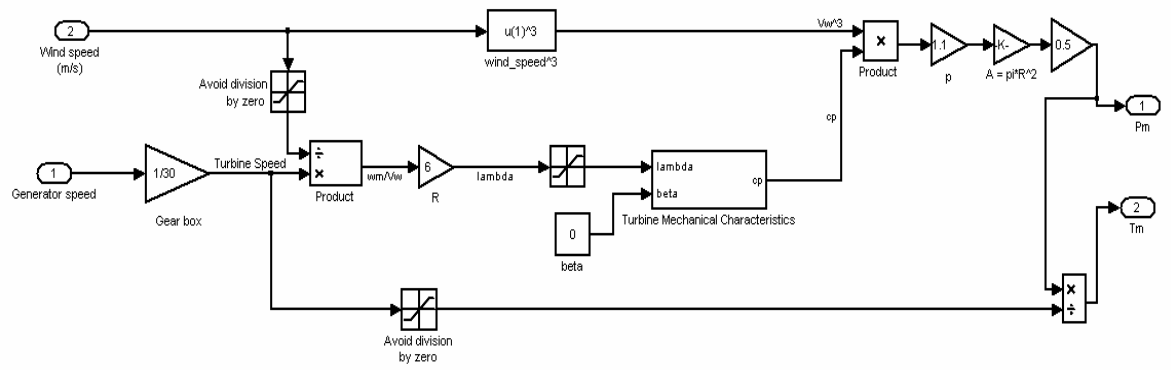

Figure 4.5: Custom Wind Turbine Structure (Air density: 1.1 kpa).

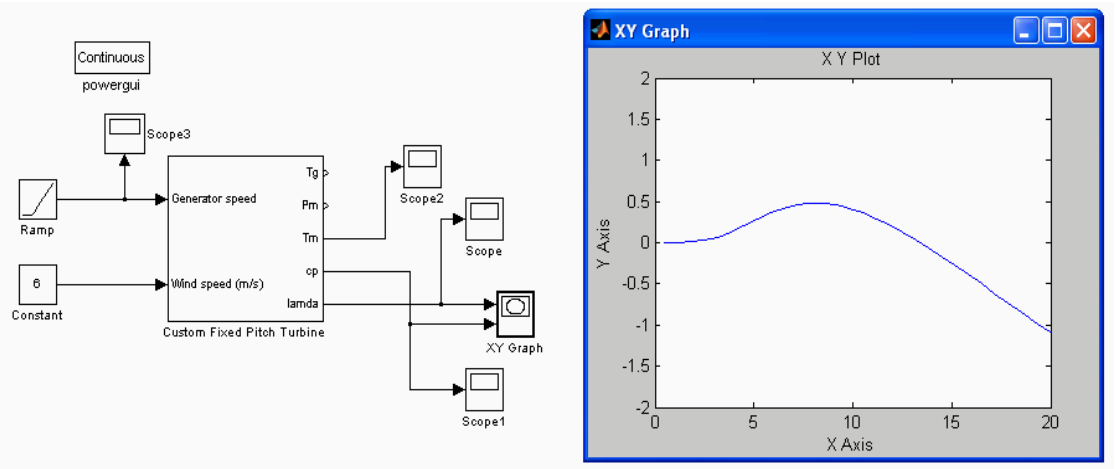

Figure 4.6: Custom Wind Turbine (Air density: 1.1 kpa).

Where T_m is the mechanical torque from the wind turbine, J_s is the total system inertia, and ω is the angular velocity of the turbine shaft. The total system inertia, J_s, is given by:

$$J_s = J_T + J_G(G) \tag{4.8}$$

Where J_T is the inertia of the turbine, J_G is the inertia of the machine, and G is the gear ratio between the turbine and the generator.

$$G = \frac{\omega_2}{\omega_1} = \frac{N_2}{N_1} \tag{4.9}$$

Figure 4.8 shows the complete wind turbine model built with PSIM 7.0 simulation software [8]. In PSIM, there is an analogy between electrical parameters (current, voltage, and capacitance) and mechanical parameters (torque, angular rotational speed, and inertia) that is used to create a custom mechanical load model. To achieve this, a dependent current source is placed in parallel with a capacitor (See figure 4.7) [8]. Figure 4.7 is an example of a custom mechanical load used with an induction machine, but it can be used for all machines in the PSIM library. The capacitor voltage

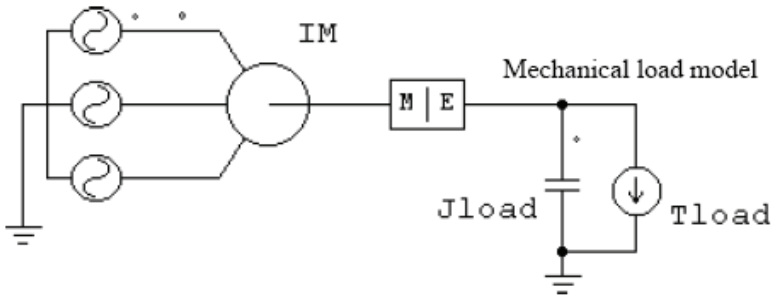

Figure 4.7: Example: An induction machine with a custom mechanical load model in PSIM [8].

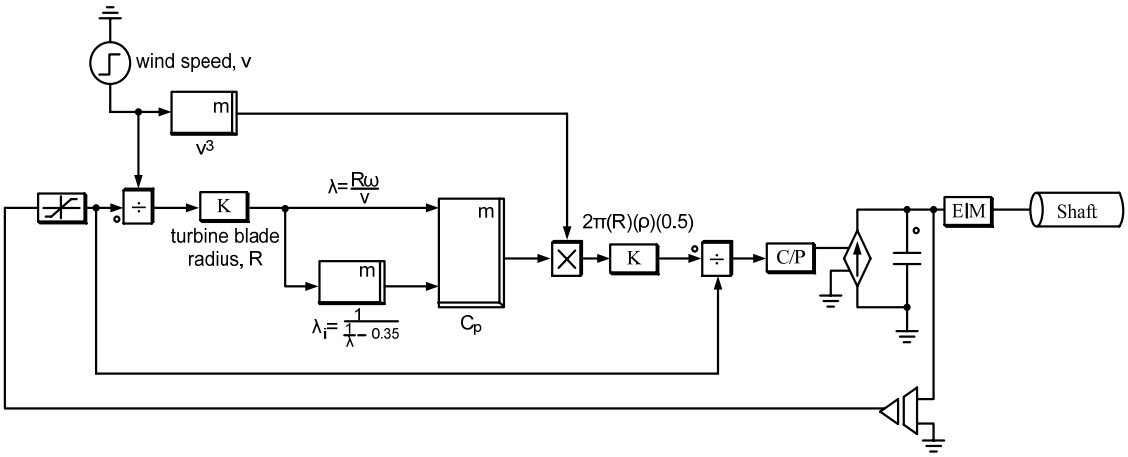

Figure 4.8: The PSIM model of the fixed-pitch turbine.

and current relationship ($i = C\frac{dv}{dt}$) is equivalent to the relationship between torque and inertia ($T = J\frac{d\omega}{dt}$). The mechanical torque, turbine inertia, and the angular rotational speed is represented by the dependent current source value, capacitance, and voltage respectively. Therefore, the capacitor value is simply changed when any modification to the turbine's inertia is necessary. The result of using this analogy allows the turbine angular speed to be applied to the turbine-generator shaft. The complete model of the wind turbine and its turbine generator shaft is illustrated by Figure 4.8.

4.2 Power Electronic Interface Analysis

To extract maximum power from the wind by varying the generator speed, a power electronics interface between the generator and the DC load side must be used to provide the system with a control parameter. Ultimately, the generator speed is controlled by changing the loading of the generator by means of the power electronic converter. As mentioned earlier in chapter 2, the two most common types of power electronics rectifiers found in WECS applications is the PWM rectifier and the single phase boost converter [27]. The advantages of using an PWM rectifier is that it does not require any inductors or capacitors in the circuit. Also, by applying PWM techniques to the rectifier, good control flexibility can be obtained. However, since the PWM rectifier requires six switches in the circuit, the control scheme would be quite complicated. Since the purpose of this thesis is to evaluate the effectiveness of the algorithm, a single phase boost converter is used. Compared to the PWM rectifier, the single phase boost converter requires only one switch in the circuit to be controlled. As a result, a simple duty ratio control loop can be used to adjust the pulse width of the switch to control the loading of the generator. Also, by operating the boost converter in discontinuous conduction mode (DCM), the boost inductor current follows the envelope of the rectified AC generator voltage and close-to-sinusoidal current can be obtained at the output of the generator. Operating the boost converter in DCM also helps to reduce the switching losses of the switch [28].

4.2.1 Design of Boost Converter

Since the main scope of this thesis is to verify the functionality of the proposed adaptive control algorithm in MPPT applications for WECS, the boost converter

is chosen as the front-end power converter connected between the PMSG and DC load side. The design specifications are listed in Table 4.2. In this design example, the boost converter was designed for the highest rated wind speed of 9 m/s. The maximum boost inductor value (L_{max}) that can be used to operate the boost converter in DCM is given by (4.10). Also, to achieve very low ripple output voltage, the minimum output capacitor value (C_{min}) is calculated by (4.11), where ΔV is 0.5% of the rated output voltage.

Table 4.2: Design specifications for boost converter.

Output Power	20kW
Load resistance (R)	20Ω
switching frequency (f_s)	5kHz
Output voltage (V_o)	632V

$$L_{max} = \frac{T_s V_o}{2I_o}(D)(1-D)^2 \tag{4.10}$$

$$C_{min} = \frac{V_o}{\Delta V}\frac{DT_s}{R} \tag{4.11}$$

For the system used in this thesis, L_{max} is calculated to be $470\mu H$ from (4.10) and C_{min} is calculated to be $600\mu F$ from (4.11). In the actual design, to ensure that the boost converter always operates in DCM under different wind conditions and that the output voltage has very low ripple, L is selected to be $200\mu H$ and C is $2000\mu F$ respectively.

4.2.2 Overall Control Concept

Figure 4.1 illustrates the overall system diagram where the MPPT block encapsulates the algorithm and the feedback control block. The system in this study uses a speed

loop control concept where the generator speed is directly compared to the reference speed generated by the MPPT block. The concept used in this thesis is based on the concept discussed in [19]. The MPPT block uses the rotor speed and the output power of the boost converter (by using the DC voltage and output current) to determine a proper speed reference. The speed error signal is obtained from comparing the reference speed and the rotor speed and is fed into the compensator. The compensator output signal is the duty ratio (d) for the boost converter. By changing d, the output power of the boost converter (and thus the generator loading) is changed.

4.2.3 Feedback Loop Analysis

The block diagram of the closed loop system is shown in Figure 4.9, where $\wedge$ represents a small signal quantity. To design a proper compensator so that all the stability requirements are met and enable the MPPT control block to accurately determine the optimum output power point for a particular wind speed, small-signal modeling of the boost converter is performed. The compensator is then designed using the SISO toolbox from MATLAB. All the relevant information including the the final closed-loop system Bode plot will be given in this section to verify all the theoretical analysis.

A. Modeling of DCM Boost Converter

Modeling of boost converter has been done extensively in literature [29][30]. The small signal model of the DCM boost converter in this design example is obtained based on the average circuit model proposed by Erickson [31]. Figure 4.10 and figure 4.11 show the corresponding average circuit model and small signal model of the boost converter respectively, where $\hat{i_1}$, $\hat{i_2}$, $\hat{i_3}$ and $\hat{i_4}$ are given in (4.12), (4.13), (4.14) and

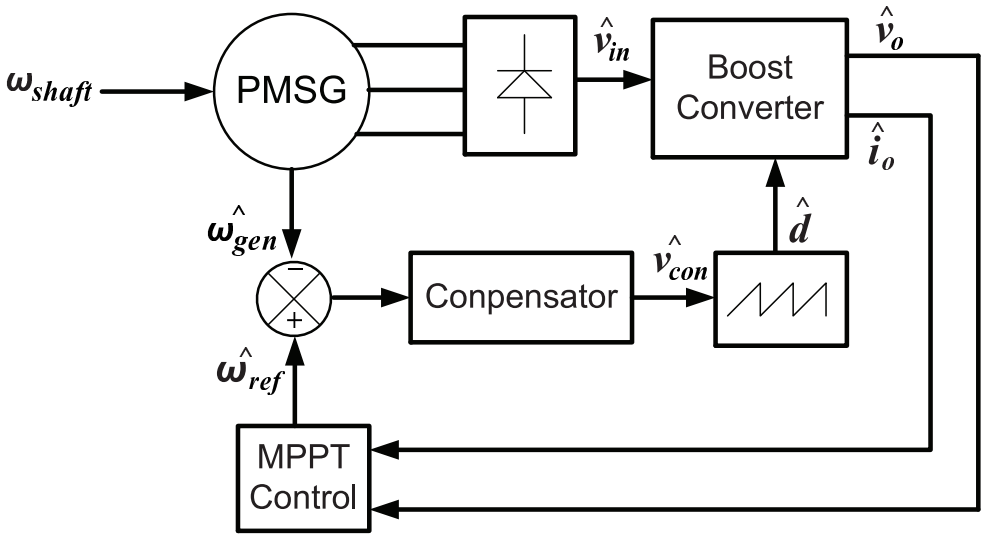

Figure 4.9: Closed loop system.

(4.15) respectively with M = V_o/V_{in}.

The control-to-output transfer function is then obtained using the circuit model shown in Figure 4.11. The final expression of $\frac{\hat{v_o}(s)}{\hat{d}(s)}$ is given in (4.16), where G_o and ω_p are given in (4.17) and (4.18) respectively.

$$\hat{i_1} = \frac{2MV_{in}}{d(M-1)R_e}\hat{d} \tag{4.12}$$

$$\hat{i_2} = \frac{v_o}{(M-1)^2R_e}\hat{v_o} \tag{4.13}$$

$$\hat{i_3} = \frac{2M-1}{(M-1)^2R_e}\hat{v_{in}} \tag{4.14}$$

$$\hat{i_4} = \frac{2V_{in}}{d(M-1)R_e}\hat{d} \tag{4.15}$$

$$\frac{\hat{v_o}(s)}{\hat{d}(s)} = \frac{G_o}{1+\frac{s}{\omega_p}} \tag{4.16}$$

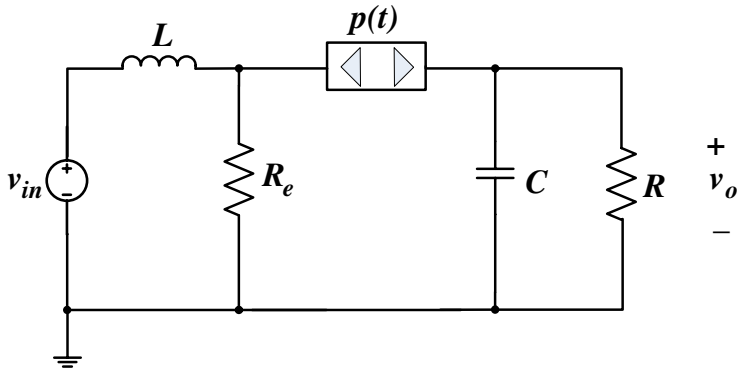

Figure 4.10: Average circuit model of DCM boost converter.

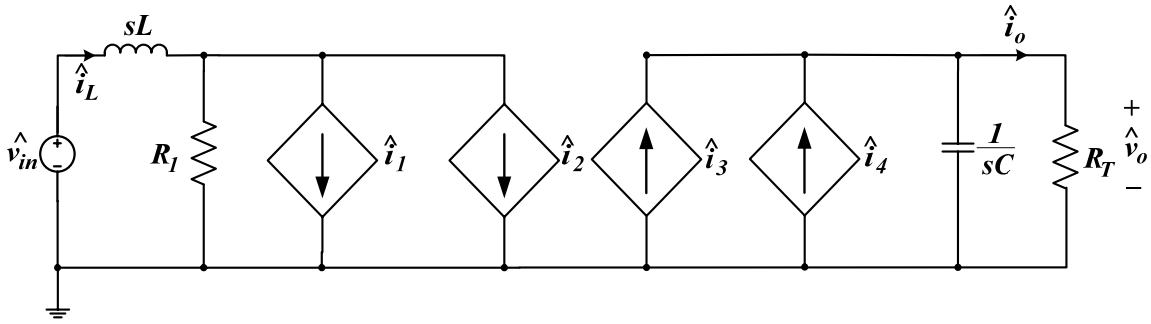

Figure 4.11: Small signal equivalent circuit of DCM boost converter.

$$G_o = \frac{2V_o(M-1)}{d(2M-1)} \tag{4.17}$$

$$\omega_p = \frac{2M-1}{(M-1)RC} \tag{4.18}$$

B. Compensator Design

Before going into the design of the compensator, the overall open loop transfer function as given by (4.19) is studied first, where the sawtooth comparator is modelled as a constant gain as given by (4.20) with $V_{pp} = 5V$. For the MPPT control block, it is observed in Figure 4.9 that the control-to-generator speed transfer function can be written as in (4.21). But with the elimination of i_o, $\hat{\omega_{gen}}/\hat{d}$ is essentially equal to control-to-output voltage transfer function multiplied by the gain between the output

voltage (v_o) and the generator speed (ω_{gen}) as shown in (4.21). Figure 4.12 illustrates the relationship between ω_{gen} and the output voltage found through system testing. The corresponding relationship is given in (4.22). It is observed that the DC output voltage (v_o) and the generator speed (ω_{gen}) presents a fairly linear relationship. In this design, a gain of 5 is obtained. The overall open-loop transfer function is then given in (4.23). It exhibits a single pole characteristic that is contributed by the DC-link capacitor. It this case, the single pole occurs at $\omega = 111.82 rad/s$ as calculated from (4.16).

$$T_{open}(s) = T_{comp}(s)T_{boost}(s)T_{\omega/v}(s) \tag{4.19}$$

$$T_{comp}(s) = \frac{1}{V_{pp}} = \frac{1}{5} \tag{4.20}$$

$$\frac{\hat{\omega_{gen}}}{\hat{d}} = \left(\frac{\hat{\omega_{gen}}}{\hat{v_o}\hat{i_o}}\right)\left(\frac{\hat{v_o}\hat{i_o}}{\hat{d}}\right) = \frac{\hat{\omega_{gen}}}{\hat{v_o}}\frac{\hat{v_o}}{\hat{d}} \tag{4.21}$$

$$T_{\omega/v}(s) = \frac{\hat{\omega}_{gen}}{\hat{v}_o} \tag{4.22}$$

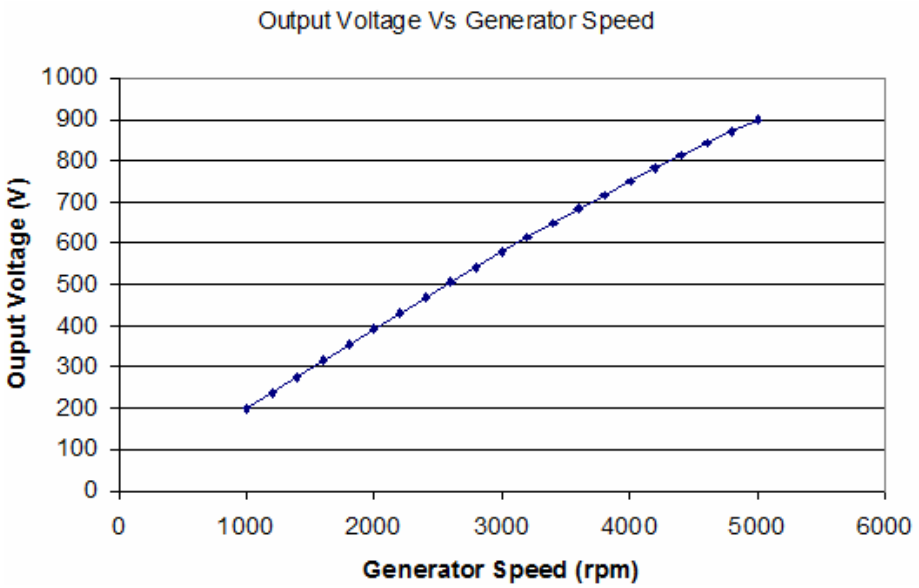

Figure 4.12: Relationship between V_o and generator speed (rpm).

In a well-regulated closed loop system, a high DC gain is essential to eliminate the steady-state error and a phase margin of at least 45^0 is recommended for a stable system . A PI compensator of the form of (4.24) is adequate to provide the required pole and zero, where k_c and T_c are the compensator gain and time constant respectively. The actual PI compensator is designed in MATLAB using the SISO toolbox. The final closed loop transfer function of the system is then given in (4.25). Figure 4.13 shows the Bode plot of the overall closed loop. It is observed that a DC gain (i.e. $\omega = 0$) of about 70dB is achieved with a crossover frequency of 400Hz and a phase margin of 65^o. The stability performance of the closed loop system will be verified through PSIM simulation in the next chapter.

$$T_{open}(s) = \frac{942}{0.008943s + 1} \tag{4.23}$$

$$T_{con}(s) = \frac{k_c(1 + sT_c)}{sT_c} \tag{4.24}$$

$$G_{closed-loop}(s) = \frac{8.312s + 4889}{0.008943s^2 + s} \tag{4.25}$$

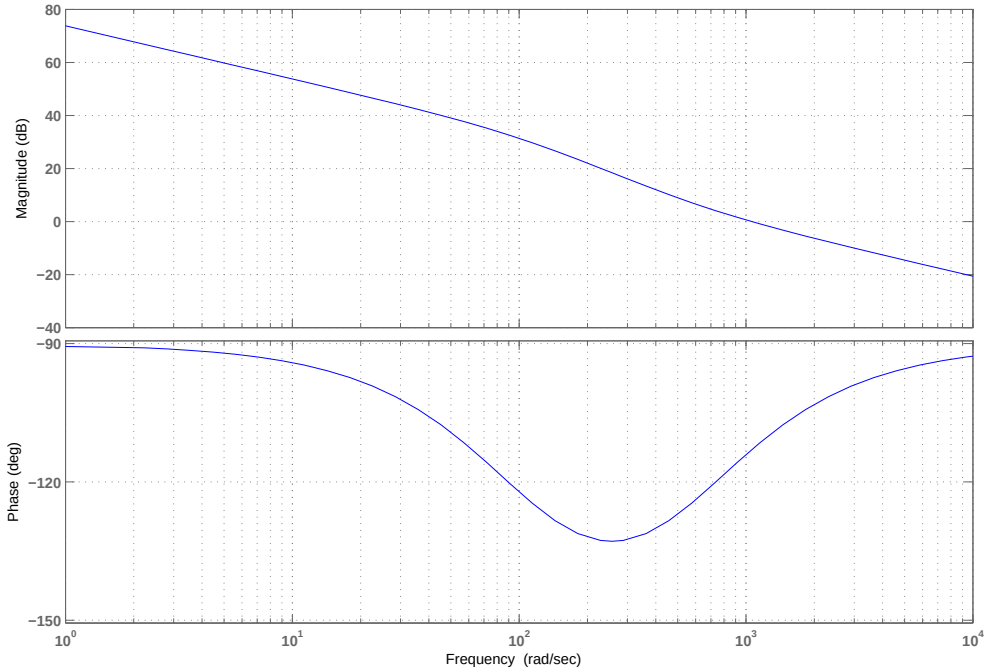

Figure 4.13: Bode plot of overall closed loop system.

Chapter 5

Algorithm Performance

5.1 Simulation Model Overview

The complete wind energy conversion system was built in PSIM 7.0, and is as illustrated in Figure 5.1. The detailed diagram of the wind turbine and turbine shaft in Figure 5.1 is given by Fig. 4.7. The C++ programmable script block is used to implement the maximum power point tracking algorithm. The algorithm requires the wind speed, generator speed, output voltage and output current as an input. Since the algorithm requires an anemometer to monitor the wind speed and calculate the turbine's internal TSR, the wind speed is directly fed into the algorithm in the simulation. The generator speed input allows the algorithm to determine whether the generator speed has reached the reference speed as desired. The output voltage and current together provides the algorithm with knowledge of the output power. Information regarding the output power, generator speed, and wind speed allow the algorithm to determine the system's maximum power points.

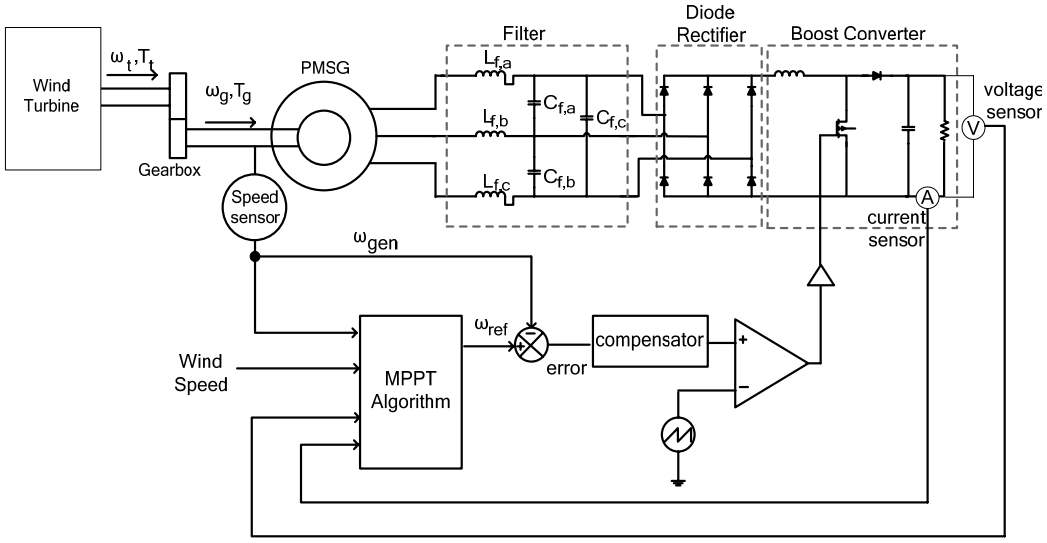

Figure 5.1: Complete wind energy conversion system.

5.2 Algorithm Operation

Figure 5.2 represents the turbine's actual power coefficient curve and it can be observed that the turbine λ_{opt} for maximum power transfer is 8.1. The power curves for wind speeds of 7 m/s and 9 m/s are given in Figure 5.3, and the optimum generator speeds are 2707 rpm and 3480 rpm respectively.

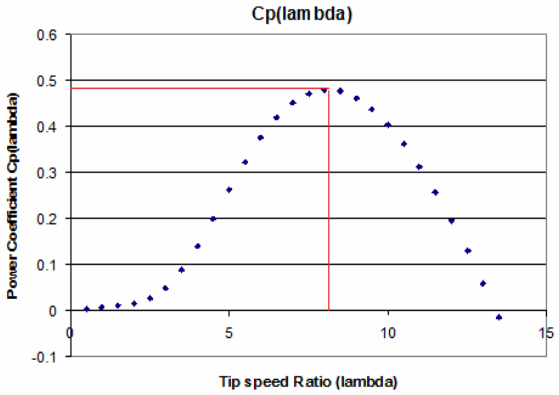

Figure 5.2: The Power Coefficient Curve of the Turbine (Optimum tip speed ratio = 8.1 as indicated).

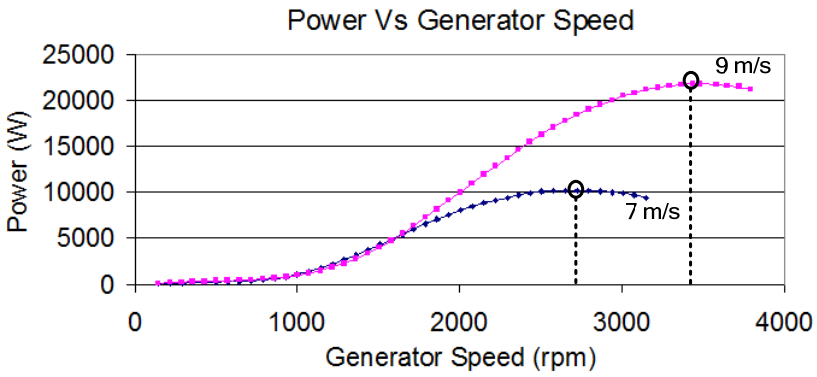

Figure 5.3: Turbine power curves for $v_w = 7$m/s and for $v_w = 9$m/s. $\omega_{opt,7} = 2707$ rpm, and $\omega_{opt,9} = 3480$ rpm.

As the algorithm progresses, its decisions to adjust the reference speed based on the operating conditions are expressed by a decision flag. Table 5.1 summarizes the meanings of each decision flag.

The concept of the proposed algorithm has been verified by using the wind energy system built in PSIM 7.0.

Figure 5.4 illustrates the maximum power point search process under a constant wind speed of 7 m/s in its initial state (the algorithm memory is empty and the generic TSR value of 7 is used). The algorithm determines an initial operating point using the TSR value, and begins it searching process. From Fig 5.4, it can be observed that the system operates at a power coefficient value of 0.45 after it reaches the first speed reference as calculated using the generic TSR value. Although the actual turbine TSR value is 8.1, the generic TSR value is able to define a starting point relatively close to maximum power point rather than beginning at an arbitrary point. The further the system operating point is from the maximum power point, the exponentially less power is extracted from the wind. By defining initial operating points using the TSR when a change in wind speed is detected, the algorithm can therefore effectively reduce

Table 5.1: The algorithm's decisions represented by values. *NOTE: flag = 3 cannot be observed in the output graphs, as it is an internal flag to invoke certain actions.

Decision Flag Value	Meaning
0	Wind speed change
1	Decrease the reference speed
2	Increase the reference speed
3*	• The change in power is within the specified limit range to consider $\Delta P \approx 0$ • Store optimum power point • Set flag = 4 to avoid any further adjustment
4	Optimum power point has been found. No adjustment to the speed is made until there has been a change in wind speed
8	The approximate optimum speed was calculated by an experimentally obtained TSR. Make a small initial adjustment.
10	Reoccurring wind speed. Use stored speed reference value from data.

the amount of lost potential wind power. The determined maximum power point for the wind speed of 7 m/s was found to be 2650 rpm, where the actual maximum power point is 2707 rpm. The corresponding rotor speeds are 9.25 rad/s and 9.44 rad/s. By substituting these speeds into (4.4), the corresponding extracted mechanical power can obtained. The power from the wind for the determined and actual optimum power point is 10226 W and 10241 W respectively. The difference in power between the determined and actual maximum power point is 15W. The power coefficient at the determined operating point was 0.4793 and the turbine's stored TSR was updated to be 7.92. The turbine's actual optimal TSR is 8.1 and the corresponding maximum power coefficient value is 0.48.

Fig. 5.5 illustrates the maximum power point search process under a constant

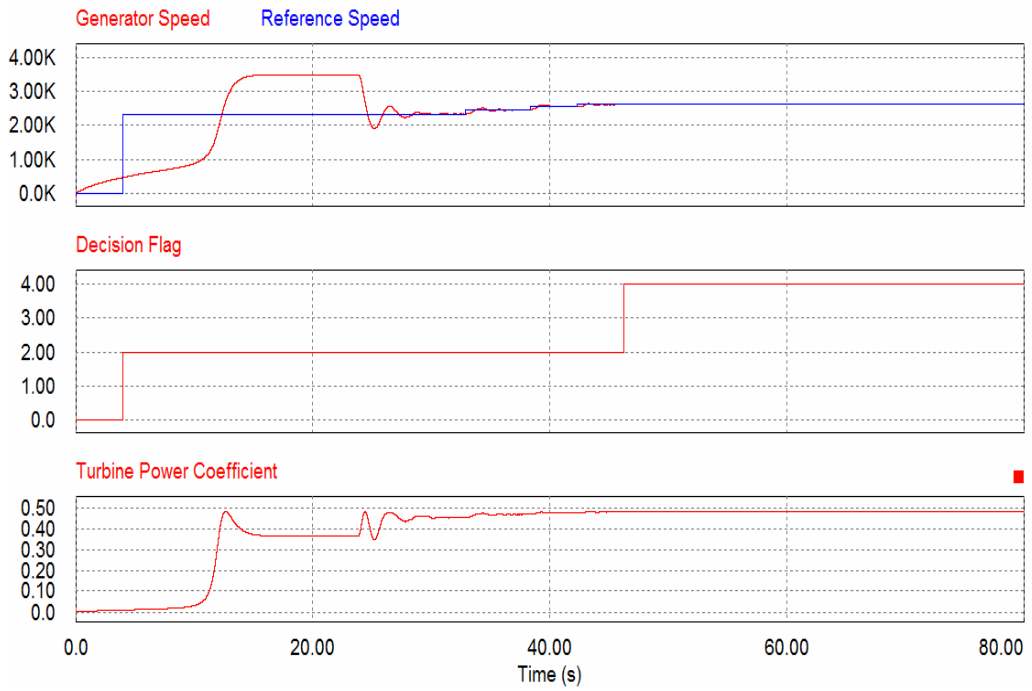

Figure 5.4: Algorithm performance under a constant wind speed of 7 m/s.

wind speed of 9 m/s in its initial state.

At a wind speed of 9 m/s, the algorithm was able to determine the generator speed to be 3381 rpm through its search procedure, while the actual maximum power point is at 3480 rpm. The corresponding rotor speeds are 11.8 rad/s and 12.1 rad/s. By substituting these speeds into (4.4), the corresponding extracted mechanical power can be determined. The power extracted by the energy conversion system at the determined and actual speeds is 21709 W and 21766 W, respectively. The algorithm is successful in determining the maximum power point of the system because the difference in power between the actual and determined operating point is 57 W (approximately 0.1% of the maximum power). The power coefficient was at 0.45 using the generic TSR value, and eventually became 0.478 at the determined maximum power point. The turbine's TSR was determined to be 0.787 which is relatively close

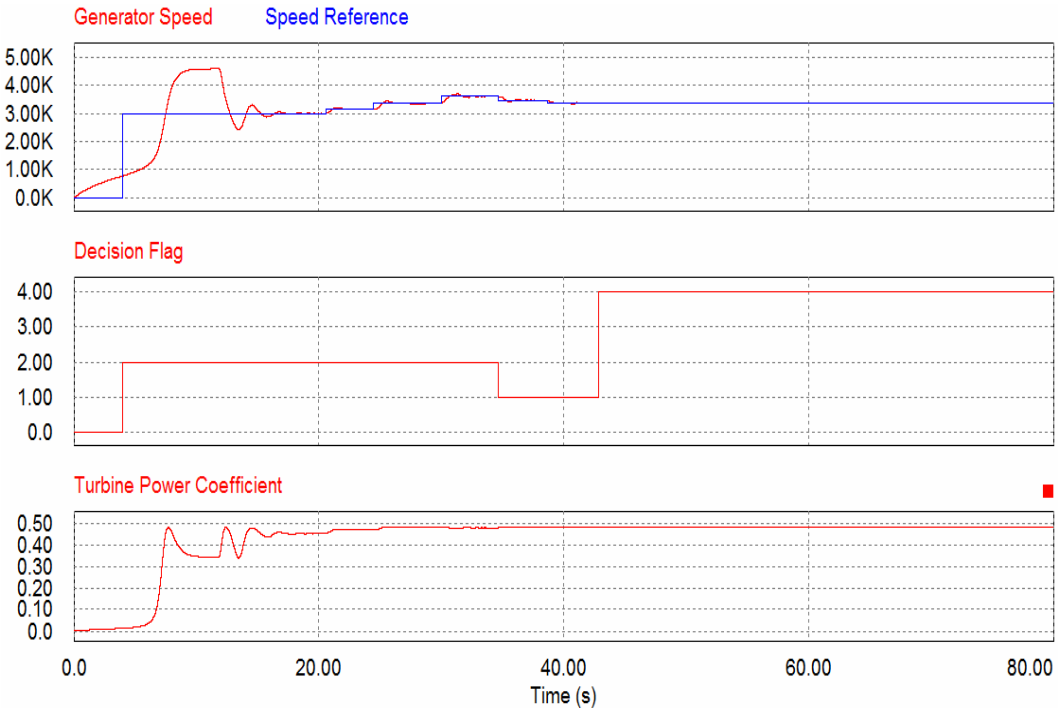

Figure 5.5: Algorithm performance under a constant wind speed of 9 m/s.

to the actual value of 8.1.

Figure 5.6 and 5.7 illustrate the benefits of the algorithm's adaptive memory. In comparison to Figure 5.5, the algorithm had to go through 5 adjustments before reaching the maximum power point. However by having the turbine's TSR calculated after an optimum power point was determined after the previous wind speed of 7 m/s, the search procedure for the new wind speed of 9 m/s was shortened to 2 adjustments. The optimum power point for 9 m/s was found to be 3441 rpm and the TSR value was updated to be 7.964 after averaging the TSR from 7 m/s and 9 m/s.

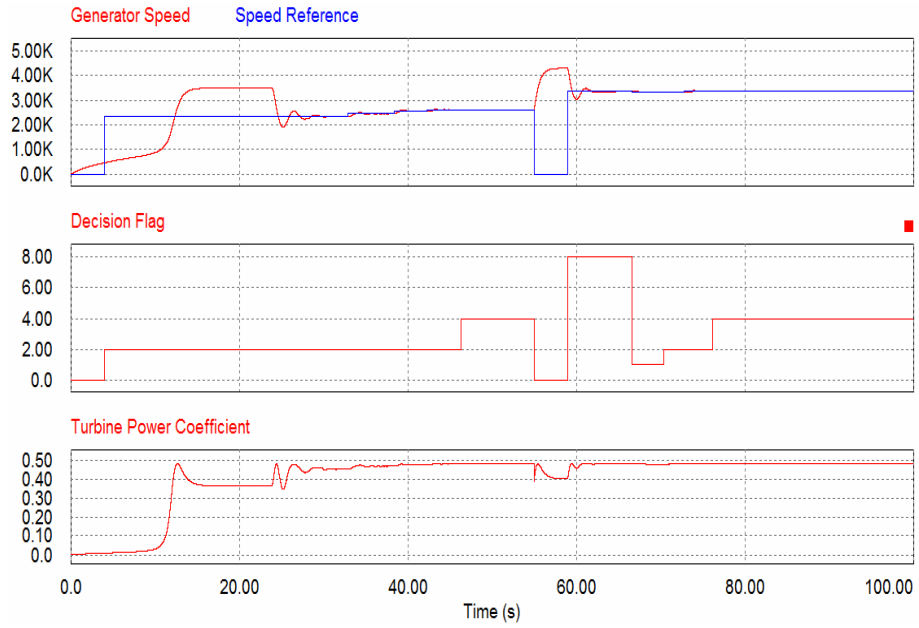

Figure 5.6: Algorithm performance under a step change in wind speed (7 m/s to 9 m/s at time = 55s).

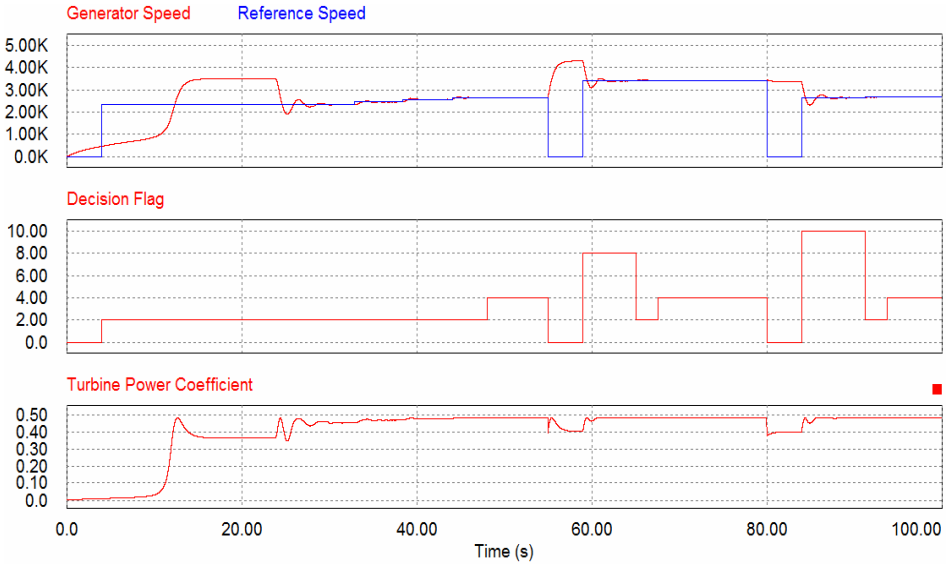

Figure 5.7: Algorithm performance under two wind speed changes (7 m/s to 9 m/s at time = 55s, 9 m/s to 7 m/s at time = 80s).

To test the algorithm's optimum point retrieval feature, the wind condition in Figure 5.7. 5.7 changes from 7 m/s to 9 m/s and then back to 7 m/s. Through simulation it was verified that when the wind speed changed back from 9 m/s to 7 m/s, the algorithm is able to retrieve and apply the stored optimum speed. As described in Chapter 3, after the algorithm applies the stored reference, it will evaluate the integrity of the stored data by introducing small speed adjustments. These small adjustments fine tune the value determined previously to obtain an even closer point to the maximum power point in the case that the data is wrong or can be improved. With the reoccurring wind speed of 7 m/s at 80s in Figure 5.7, the algorithm was applied the stored optimum speed of 2650 rpm and subsequently small adjustments were made. Through the small adjustments, the stored maximum power point value was further fined tuned to a more accurate value of 2676 rpm and the TSR value was updated to 7.977 (See Figure 5.9).

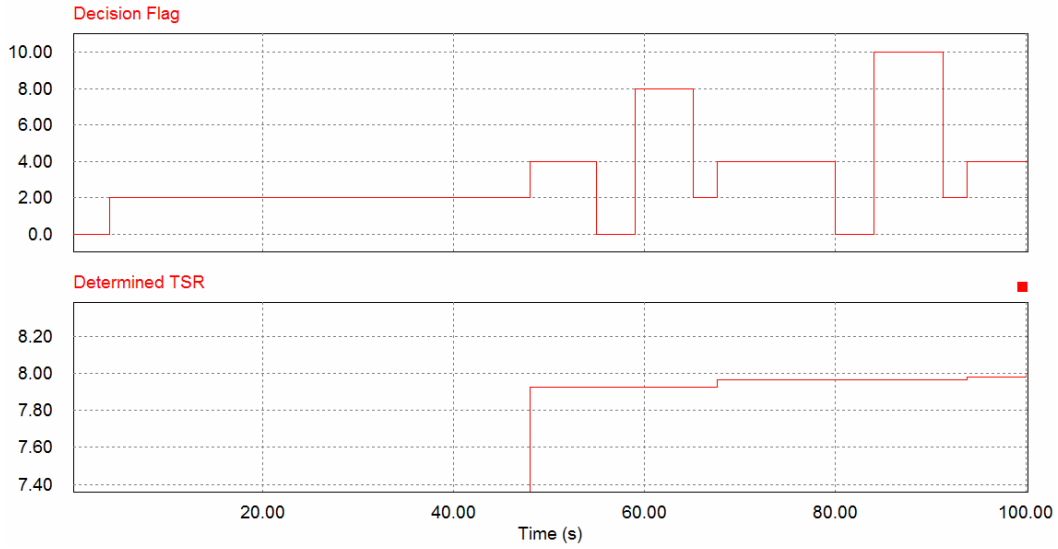

Figure 5.8: Illustration of the algorithm's TSR determination process under two wind speed changes (7 m/s to 9 m/s at time = 55s, 9 m/s to 7 m/s at time = 80s).

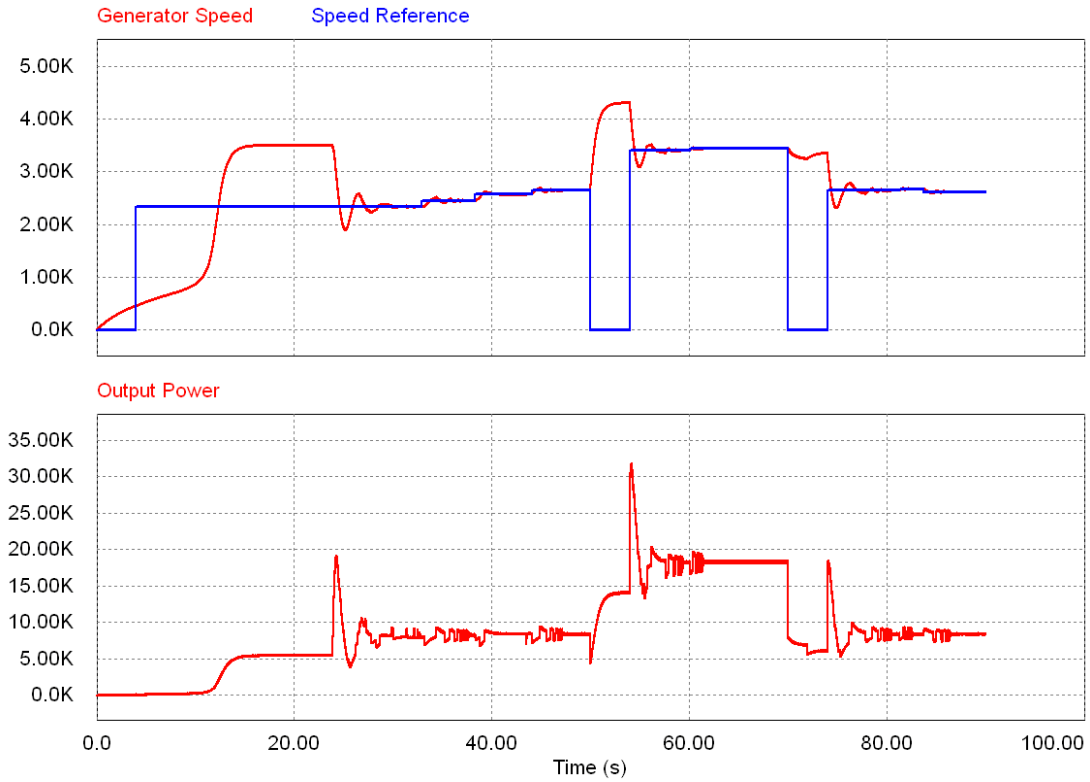

Figure 5.9: Illustration of the algorithm's optimum point determination process (speed adjustment and output power) under two wind speed changes (7 m/s to 9 m/s at time = 55s, 9 m/s to 7 m/s at time = 80s).

5.3 Results Summary

Through simulation it has been shown that the algorithm is capable of finding the maximum power point of a wind energy system and adapting to a wind turbine's optimal TSR. Furthermore, the algorithm's implemented memory and power management scheme is effective in reducing the amount of search procedures with each optimum point determination. It can also be observed that the algorithm is successful in controlling the system to mainly operate near its maximum power coefficient value to minimize the loss of potential wind energy.

Chapter 6

Summary and Conclusions

6.1 Summary

With rising concerns over rising energy prices, depletion of natural resources and pollution, environmentally friendly energy resources like wind energy are becoming more prominent. Wind energy is inexhaustible, safe, has no harmful by products and is capable of supplying substantial amounts of power. The unpredictable availability of wind however, only allows it to become a secondary source of power. In order to harness as much power from the wind as possible while it is available, intelligent control strategies must be implemented. With technological advancements in wind turbine aerodynamics and power electronic interfaces, wind energy can be considered to be an excellent renewable supplementary energy source. Power electronic interfaces and intelligent control strategies make wind energy viable and attractive despite its intermittent availability.

This thesis provides extensive background knowledge on the wind energy market, turbine technology, and energy conversion. The main purpose of this thesis is to

design and develop an algorithm to enable maximum power transfer under fluctuating wind conditions. Various algorithms and control schemes that attempt to extract the maximum power from the wind were studied and presented. The concepts were grouped into three main categories: i) customized, ii) continual adjustments, iii) adaptive. The study identified the main problems in existing maximum power point extraction algorithms, and then used them as guidelines for the algorithm design. The main problems are customization, speed, and wasted power. The customization problem refers to the preprogramming of a turbine's characteristic into an algorithm, making it effective only for the turbine it was originally designed for. The decisions and structure of each customized algorithm is based on the turbine characteristics and each wind turbine has its distinct characteristic. Therefore, customized algorithms cannot be easily reused onto other turbines and it would be costly to continually design a new algorithm. The speed of the algorithm has a great effect on the amount of wasted potential wind power. A wind turbine does not naturally operate at its most efficient operating point, and due to the shape of wind turbine power curves, a significant amount of wind power can be left unharnessed. As a solution to these problems, the proposed algorithm uses a modified version of an established concept known as the hill climb search (HCS) algorithm. The modified concept uses the standard concept in conjunction with intelligent memory and power management schemes to enable the algorithm to quickly determine maximum power points and adapt to any given turbine.

Since literature did not provide methods for the design of a complete wind energy conversion system, the system used in this thesis was built to resemble those in literature. A wind energy conversion system with a custom wind turbine was constructed

based on the wind turbine model in MATLAB Simulink. The generator was directly incorporated into the system by using the model provided by PSIM, and the PMSG parameters were based on literature values. In order to build the system for easy algorithm verification, the boost converter configuration was used. The boost converter configuration is a common method used in variable speed PMSG wind turbine applications [6][8][19]. To ensure that the system exhibited characteristics that were similar to the wind energy system found in literature, extensive tests were performed.

6.2 Contributions

The main contributions of this thesis are summarized as follows:

1. The proposed algorithm structure incorporates intelligent memory to achieve unsupervised training. Because the optimal TSR that corresponds to a maximum power coefficient for all wind speeds, the unsupervised training is achieved by using the maximum power point search data to determine an experimentally TSR value.

2. The algorithm is easily configured for any given wind turbine because it does not require previous knowledge or the turbine characteristics or the wind energy conversion system configuration to make its decisions. The algorithm is structured so that the internal turbine characteristics are determined through operation. Although a TSR value is used in the initial stage of the algorithm, it is a generic optimum TSR for a horizontal-axis, three-blade wind turbine

3. Maximum power can be quickly extracted under wind fluctuations due to the use of the TSR relationship. By using the TSR relationship, the algorithm can

immediately jump to an operating point very close to the maximum power point rather than operating an arbitrary point depending on the systems operating conditions. With the added memory in the system, the algorithm is also capable of jumping to the maximum power point in the case of a reoccurring wind speed. This allows the system to bypass any redundant search procedures and therefore minimizes the loss in potential power.

4. A complete wind energy system has been designed in this thesis. The modeling of the wind turbine to the DC-DC converter for a front-end rectifier wind energy system is provided.

6.3 Future Works

Future works related to the proposed circuit could be summarized as follows:

1. Experimental verification of the proposed algorithm by using a low power wind turbine. The proposed algorithm can be implemented by using field programmable gate array (FPGA) techniques or digital signal processors (DSP).

2. A new algorithm that can provide comparable performance without the use of an anemometer, can be developed. Sensorless wind energy systems are more cost effective and robust.

3. Different converter topologies can be implemented to provide better control. Such as matrix converters and PWM rectifiers.

4. In this thesis, the proposed algorithm is tested under step changes in wind. To obtain more practical performance results to further improve on the design, a

wind prediction scheme can be developed to model realistic wind behavior.

6.4 Conclusion

Due to wind's unpredictable nature, power management concepts are necessary to extract as much power as possible from the wind when it becomes available. The proposed algorithm has been developed to maintain the system at its highest possible efficiency by using its memory feature to infer the optimum rotor speeds for wind speeds that have not occurred before. Another feature of the proposed algorithm is that it can be easily customized for various wind turbines since it is independent of turbine characteristics. The proposed algorithm uses a modified version of HCS and intelligent memory to implement its power management scheme. This algorithm is most suitable for smaller grid or battery connected wind energy systems. PSIM simulation studies have confirmed the effectiveness of the proposed algorithm.

Bibliography

[1] "Global wind 2007 report," May 2008.

[2] "Global wind 2006 report," June 2007.

[3] M. Idan, D. Lior, and G. Shaviv, "A robust controller for a novel variable speed wind turbine transmission," *Journal of Solar Energy Engineering*, vol. 120, pp. 247–252, 1998.

[4] R. Gilbert, "Regulatory choices: A perspective on developments in energy policy," *Mathematical and Computational Applications*, pp. 10–17, December 2007.

[5] S. Muller, M. Deicke, and R.-W. De Docker, "Adjustable speed generators for wind turbines based on doubly-fed induction machines and 4-quadrant igbt converters linked to the rotor," *IEEE Industry Applications Conference*, vol. 4, pp. 2254–2259, October 2000.

[6] J. Marques, H. Pinheiro, H. Grundling, J. Pinheiro, and H. Hey, "A survey on variable-speed wind turbine system," *Proceedings of Brazilian conference of electronics of power*, vol. 1, pp. 732 – 738, 2003.

[7] Q. Wang and L.-C. Chang, "An intelligent maximum power extraction algorithm for inverter-based variable speed wind turbine systems," *IEEE Transactions on Power Electronics*, vol. 19, pp. 1242–1249, September 2004.

[8] P. Inc, *PSIM: User Manual*. Powersim Inc., 1 ed., 2001.

[9] T. I. of Electrical and E. E. Inc, "Ieee canadian review: Green power," *Mathematical and Computational Applications*, pp. 10–17, December 2007.

[10] C. W. E. Association, "Wind facts - an introduction to wind power," *Mathematical and Computational Applications*, 2007.

[11] F.-S. dos Reis, K. Tan, and S. Islam, "Using pfc for harmonic mitigation in wind turbine energy conversion systems," *IEEE Industrial Electronics Society Conference*, pp. 3100–3105, November 2004.

[12] "windpower.org," 2006.

[13] G. Moor and H. Beukes, "Power point trackers for wind turbines," *Power Electronics Specialist Conference (PESC)*, pp. 2044–2049, 2004.

[14] Y. Song, B. Dhinakaran, and X. Bao, "Variable speed control of wind turbines using nonlinear and adaptive algorithms," *Journal of Wind Engineering and Industrial Aerodynamics.*, vol. 85, no. 3, pp. 293–308, 2000.

[15] D.-S. Zinger and E. Muljadi, "Annualized wind energy improvement using variable speeds," *IEEE Transactions on Industry Applications*, vol. 33, pp. 1444–1447, November 1997.

[16] M. Chinchilla, S. Arnaltes, and J.-C. Burgos, "Control of permanent-magnet generators applied to variable-speed wind-energy systems connected to the grid," *IEEE Transactions on Energy Conversion*, vol. 21, pp. 130–135, March 2006.

[17] E. Koutroulis and K. Kalaitzakis, "Design of a maximum power tracking system for wind-energy-conversion applications," *IEEE Transactions on Industrial Electronics*, vol. 53, April 2006.

[18] T.-S. Shikha, Bhatti, and D.-P. Kothari, "A new vertical axis wind rotor using convergent nozzles," *Large Engineering Systems Conference on Power Engineering*, pp. 177–181, May 2003.

[19] I. Munteanu, A. I. Bratcu, N. Cutululis, and E. Ceanga, *Optimal Control of Wind Energy Systems: Towards a Global Approach.* Springer-Verlag London Limited, 1 ed., 2008.

[20] F. Blaabjerg and Z. Chen, *Power Electronics for Modern Wind Turbines.* Morgan & Claypool Publishers, 1 ed., 2006.

[21] S. Bhowmik, R. Spee, and J.-H.-R. Enslin, "Performance optimization for doubly fed wind power generation systems," *IEEE Transactions on Industry Applications*, vol. 35, pp. 949–958, July/August 1999.

[22] R. Datta and V.-T. Ranganathan, "A method of tracking the peak power points for a variable speed wind energy conversion system," *IEEE Transactions on Energy Conversion*, vol. 18, pp. 163–168, March 2003.

[23] T. Nakamura, S. Morimoto, M. Sanada, and Y. Takeda, "Optimum control of ipmsg for wind generation system," *Power Conversion Conference (PCC)*, vol. 3, pp. 1435–1440, 2002.

[24] N.-S. Cetin, M.-A. Yurdusev, R. Ata, and A. Ozdemir, "Assessment of optimum tip speed ratio of wind turbines," *Mathematical and Computational Applications*, vol. 10, pp. 147–154, March 2005.

[25] A.-B. Raju, K. Chatterjee, and B.-G. Fernandes, "A simple maximum power point tracker for grid connected variable speed wind energy conversion system with reduced switch count power converters," *IEEE Power Electronics Specialist Conference, PESC '03*, pp. 748 – 753, June 2003.

[26] "Wind turbine model," 2006.

[27] C. Silva, R. Bascope, and D. Oliveira, "Three-phase power factor correction rectifier applied to wind energy conversion systems," *Applied Power Electronics Conference and Exposition, 2008. APEC 2008.*, pp. 768 – 773, Feb 2008.

[28] K.-H. Liu and Y.-L. Lin, "Current waveform distortion in power factor correction circuits employing discontinuous-mode boost converters," *Power Electronics Specialists Conference*, pp. 825 – 829, June 1989.

[29] Y.-F. Liu and P.-C. Sen, "A general unified large signal model for current programmed dc-to-dc converters," *IEEE Transactions on Power Electronics*, pp. 414 – 424, July 1994.

[30] J. Sun, D. Mitchell, M. Greuel, P. Krein, and R. Bass, "Modeling of pwm converters in discontinuous conduction mode. a reexamination," *Power Electronics Specialists Conference, 1998. PESC 98*, pp. 615 – 622, May 1998.

[31] E. Rogers, "Application note: Understanding boost power stages in switch mode power supplies," *Texas Instruments*, pp. 1–32, March 1999.